4.1 INTRODUCTION

Cytokines are low molecular weight glycoproteins produced by myriad cell types, predominantly leukocytes, which regulate various physiological and pathological functions including innate and adaptive immunity in addition to plethora of inflammatory responses. Redundancy, synergy, and pleiotropism are the characteristics of cytokine action and provide accountability for the effectiveness of these proteins in regulating immune response (Kuby, Immunology, 6th Ed., 2007). Vitiligo is a hypo-pigmentary skin disorder caused due to selective destruction of melanocytes of poorly understood etiology. There is growing evidence that cytokines play an important role in the depigmentation process of vitiligo (Moretti *et al*., 2002; Moretti *et al*., 2009). Cytokines such as IL1, IFN-γ or TNF-α released by lymphocytes and keratinocytes can initiate apoptosis of melanocytes. Also, TNF-α, IL1-α, IL6, and TGF-β are potent inhibitors of melanocyte growth (Swope *et al*., 1991; Moretti *et al*., 2002). Previous studies, including ours, have shown increased levels of TNF-α, TNF-β, IFN-γ, IL4, IL1-β and ICAM1 in vitiligo patients (Laddha *et al*., 2012; Laddha *et al*., 2013; Dwivedi *et al*., 2013; Imran *et al*., 2012; Laddha *et al*., 2014; Tu *et al*., 2003; Badri *et al*., 1993). Therefore, it becomes pertinent to investigate the effect of these cytokines in melanocyte biology. The modulation of inflammatory phenomena and immune response including restoration of the keratinocyte-melanocyte axis with specific low dose of interleukins, antibodies and basic fibroblast growth factor represent an innovative therapeutic approach for vitiligo treatment. Exploring this avenue will substantiate the basis of 'low dose cytokine therapy' for vitiligo (Lotti, 2015). To develop effective treatment modality for melanocyte related disorders such as vitiligo, melanoma etc. it is essential to understand the biology of melanocyte, especially its primary function i.e., melanin synthesis. Hence, we aimed to explore the effect of TNF-α, IL-6, IL-1α and IL-10 on the melanocyte biology by monitoring cell viability, melanogenesis [Tyrosinase *(TYR)* and Microphthalmia Associated Transcription Factor *(MITF)-M*] and *ICAM1* expression levels upon exogenous stimulation of primary cultured normal human melanocytes (NHM) with different cytokines.

4.2 MATERIALS AND METHODS

4.2.1 Ethics statement It is stated in Chapter II.

4.2.2 Study subjects (Histopathological studies)

This case–control study was carried out on 6 vitiligo patients and controls. Vitiligo patients were selected from the Dermatology Unit of Seth Vadilal Sarabhai Hospital, Ahmedabad. The disease duration in patients was ranging from 6 months to 50 years. The control group consisted healthy individuals, without any history of auto-immune or skin related diseases with an age range from 20 to 50 years old. Vitiligo was clinically classified according to Taieb and Picardo, 2007. The importance of the study was explained to all participants and written consent was obtained. Demographic details of the subjects recruited and sample details are provided in Table 1.

Table 1: Demographic details of control and vitiligo patients (Histopathological studies)

	Control (n=6)	**Patient (n = 6)**
Sex (Men: Women)	2:4	1:5
Age, mean (range), yrs	25.86 ± 4.728	34.43 ± 5.173
Duration of lesions	NA	13.0 ± 6.633 months
Size of lesions	2-10 cm in diameter	2-10 cm in diameter
Type of Vitiligo	NA	
Segmental Vitiligo	-	3
Non-segmental Vitiligo	-	3
Sites	Breast, Abdomen and Foreskin	Head and neck, trunk and the extremities.

4.2.3 Skin biopsies

From each patient, 5-mm punch biopsy collected after applying 2% lignocaine (a local anesthesthetic agent). In vitiligo patients, skin biopsies were taken from three regions: non-lesional, peri-lesional and lesional. Here non-lesional is the normal appearing skin of vitiligo patient, peri-lesional is the active border of the depigmented patch and lesional is the depigmented patch of the skin of vitiligo patient. All specimens were fixed in 10% neutral-buffered formalin and subjected to routine tissue processing that ended with paraffin-embedded blocks ready for sectioning. Hematoxylin and Eosin (H and E)-stained sections were examined microscopically to evaluate pathological changes in epidermal and dermal region.

4.2.4 Epidermal thickness and rete ridges pattern

The sections were randomly examined and photographed with Nikon D100 digital camera at low magnification (20X) under a microscope (Olympus, Tokyo, Japan). Viable epidermal thicknesses were measured at 10 different points including the thickest and the thinnest areas of each section with the exception of follicles using a computerized image analyzer (Image-J software). The viable epidermis was defined from the top of the stratum granulosum or from the top of the stratum lucidum in the case of palms and soles to the base of the stratum basale. The pattern of rete ridges was observed between non-lesional, peri-lesional, lesional and control skin under the microscope.

4.2.5 Hematoxylin and Eosin stain (Baker, 1962)

Hematoxylin and eosin staining were performed for 6 vitiligo patients and 6 controls. Skin biopsies were fixed in a 10% buffered formalin solution, processed, and embedded in paraffin. Paraffin blocks were cut into 4- to 5-micron sections on a microtome and placed on glass slides coated with Poly-L-Lysine. Sections were deparaffinized by giving 2 changes of xylene, 10 mins each. Sections were hydrated once in absolute alcohol for 5 mins followed with 95% alcohol for 2 mins and 70% alcohol for 2 mins followed by brief wash with distilled water.

The slides were then washed briefly in distilled water and stained with Harris hematoxylin (BHI, Hi-Media, India) solution for 8 minutes and then wash in running tap water for 5 minutes. The differentiation step was carried out in 1% acid alcohol for 30 seconds followed by a wash under running tap water for 1 minute. Subsequently, the bluing of the sections was done in 0.2% ammonia water or saturated lithium carbonate solution or under running tap water for 30 seconds to 1 minute. The slides were washed under running tap water for 5 mins and rinsed in 95% alcohol, 3mins/10dips. Eosin-phloxine (BHI, Hi-Media, India) solution was used to counter stain for 30 seconds to 1 minute. Lastly the slides were dehydrated through 95% and, absolute alcohol, 5 minutes each and clear in 2 changes of xylene, 5 minutes each. The sections were mounted with Xylene/DPX based mounting medium. The sections were examined randomly and photographed with Nikon D100 digital camera at low magnification (20X) under a microscope (Olympus, Tokyo, Japan).

4.2.6 Immunohistochemical studies

Skin biopsies were fixed in 10% buffered formalin solution, processed, and embedded in paraffin. Paraffin blocks were cut into 4 to 5micron sections using a microtome and placed on glass slides coated with Poly-L-Lysine. Deparaffinization of the sections was done in xylene and rehydration in a graded series of alcohol was carried out. The sections were then washed in PBS for 5 mins and then permeabilization of the sections was done with PBST (0.1% triton X / tween 20) for 15 mins followed by wash by PBS for 5 mins.

Antigen retrieval for demasking of antigens was carried out by boiling the slide in citrate buffer (pH 6.0)/Tris-EDTA (pH 9.0) using a microwave oven for three cycles, 5 mins each with a 1-min break between each cycle. After cooling to room temperature, the slides were washed twice with PBS-buffer (pH 7.4). The blocking of non-specific interactions was accomplished by incubating the samples with blocking serum (5% BSA) for 30 min at room temperature. For immunofluorescence studies, the sections were probed overnight at 4^0C with anti-MITF mouse monoclonal antibody (Abcam, ab19139, Cambridge, MA) at a dilution of 1:400. After thorough washes in PBS for three times, 5 mins each, the sections were incubated with their respective Cy3 conjugated anti-mouse IgG secondary antibodies (1:200) (Invitrogen, Carlsbad, CA, United States) for 1 hr, and wash with PBS for three times, 5 mins each. 30-40µL of the diluted DAPI solution was added to each well and incubated for 10-15 mins at room temperature. DAPI binds to DNA and is a convenient nuclear counter stain. It has an absorption maximum at 358 nm and fluoresces blue at an emission maximum of 461 nm. The sections were mounted using cover slip with anti-fading medium and the confocal imaging was carried out on a FV1000-D (Olympus, Tokyo, Japan) confocal laser 0020 scanning microscope. Excitation and detection of the samples were carried out in sequential modes to avoid overlapping of signals. The sections were scanned simultaneously at both wavelengths (555/580 nm) with appropriate laser intensity, confocal aperture, and gain. The Black-level setting was kept constant for all the samples**.**

4.2.7 Ethics statement & Culture establishment of primary normal human melanocytes (NHM) These aspects are described in Chapter II.

4.2.8 MTT assay

The number of viable cells was recorded using MTT [3-(4,5-dimethyl thiazol-2-yl)-2,5-diphenyl tetrazolium salts] (Mosmann, 1983). NHM were seeded in 96-well plates at an initial density of 5×10^3 cells per well and after overnight incubation, the cells were treated with human recombinant cytokines: TNF-α, IL-1α, IL-6, and IL10 in a dose dependent manner (0, 10, 50, 100 ng/ml). After 48 hrs of treatment, MTT (Molecular probes® by Life Technologies™, China) was added to each well and the cells were incubated at 37°C for 4 hrs. The medium was removed and dimethyl sulfoxide (DMSO) (Sisco Research Laboratories, Mumbai) was added to dissolve the formazan crystals. The absorbance was measured at 570 nm using ELISA plate reader (Thermo Scientific Multiskan EX, Shanghai, China).

4.2.9 Melanin content assay (Hu, 2008)

NHM were cultured in 6-well plates at a concentration of 1×10^5 cells/well overnight and then treated with TNF-α for 48 hrs. Then the cells were trypsinized and counted. The same number (1×10^5) of cells were collected and the pellets were dissolved in 1 M NaOH at

80°C for 1 hr. Melanin concentrations were measured by absorbance at 470 nm. The results are the compilation of three independent experiments.

4.2.10 Analysis of complex-I activity (Prajapati *et al*., 2015)

Complex-I activity of electron transport chain was determined by Spectrophotometry. The activity of complex-I was determined using decyl ubiquinone as the electron acceptor and NADH as the donor. Briefly, cells were harvested and washed with cold DPBS. Cells were subjected to freeze-thawing two or three times in Freeze–Thaw complete solution (0.25 M Sucrose, 20 mM Tris–HCl (pH 7.4), 40 mM KCl, 2 mM EDTA supplemented with 1 mg/ml fatty acid-free BSA, 0.01% Digitonin and 10% Percoll). After completion of the freeze-thawing process, the cells were washed with Freeze–Thaw solution devoid of digitonin to remove the residual digitonin as it interferes with the complex-I enzyme assay. Cells were suspended in complex-I assay buffer (35 mM Potassium Phosphate (pH7.4), 1 mM EDTA. 2.5 mM NaN_3, 1 mg/ml BSA, 2 μg/ml Antimycin A and 5mM NADH). Complex-I activity was measured for 3 mins by following the decrease in absorbance at 340 nm after the addition of 2.5 mM decyl ubiquinone indicating the oxidation of NADH.

4.2.11 Cellular and Mitochondrial reactive oxygen species (ROS) estimation

In order to observe the formation of reactive oxygen species, a fluorescent dye 2',7' dichlorodihydrofluorescein diacetate (H_2DCFDA-AM) was used. Oxidation of H_2DCFDA by ROS converts the molecule to 2',7' dichlorodihydrofluorescein (DCF), which is highly fluorescent. Upon stimulation, the resultant production of ROS causes an increase in fluorescence over time. $1x10^6$ cells were harvested and washed with 1X PBS twice. DCFDA (50 nM) was added to the cells and was incubated for 15 min at 37^0C with shaking, followed by two washes with 1X PBS. Fluorescence was measured by flow cytometry (BD Biosciences FACS-ARIA III) using 200 µl sample diluted 5 times using 1X PBS. Excitation (λex) and emission (λem) wavelengths used for fluorimetric studies were 480 and 525 nm respectively (Esposti, 2002). Similarly, 5µM MITOSOX dye which specifically measures mitochondrial ROS levels with an excitation wavelength of 510 nm and an emission wavelength of 580 nm was used.

4.2.12. Monitoring MITF-M levels upon cytokine stimulation by immunofluorescence

MITF-M antibody at a concentration of 0.5 µg/100µl (1:200, Abcam 80651) and anti-mouse IgG (whole molecule) TRITC conjugate (Sigma) at a dilution of 1:400 were used to study MITF-M expression upon cytokine stimulation. NHM were seeded on a coverslip ($0.4x10^6$ cells/ well) in a 6 well plate and incubated overnight at 37^0C with 5% CO_2 in a humidified incubator. After overnight incubation, cytokine treatment was given along with media replacement and the cells were further incubated for 48 hrs. After treatment, cells were washed once with phosphate buffered saline (PBS) pH 7.4, fixed in 70% chilled methanol for 10 min at -20°C and then washed with blocking solution (1.5% BSA with 0.05% Tween 20 in PBS), incubated for 8 hrs in primary antibody. After incubation, the cells were washed 2-3 times with blocking solution and further incubated for 1 hr with TRITC labeled secondary antibody. Followed by 2 PBS washes, cells were observed for fluorescence which was monitored under 63X by Zeiss confocal laser scan fluorescence-inverted microscope (LSM 710; Carl Zeiss). Data were analyzed using Image Pro plus software to calculate mean density of fluorescence and graphs were plotted using Graph Pad prism software.

4.2.13 Western Blot analysis

To detect alterations in protein levels, NHM were treated with or without TNF-α. Total cell lysates were obtained by Laemmli Buffer (10% SDS, 0.0625 M Tris-HCl, pH 6.8, 10% glycerol, and 5% 2-beta-mercaptoethanol) extraction. Thirty µg of total protein was subjected to electrophoresis in 12.5% SDS gel under reducing conditions and subsequently transferred to polyvinylidene difluoride (PVDF) membranes (Hybond-P, Amersham Pharmacia Biotech, Piscataway, NJ, USA). The membranes were incubated with the following antibodies: TNFR1, MITF, caspase 3, LCI-II and β-actin. Protein bands were detected by enhanced chemiluminescence system ECL (Amersham Pharmacia Biotech) and densitometric analysis was carried out with β-actin as a loading control.

4.2.14 RNA extraction and cDNA synthesis

Total RNA from primary NHM was isolated and purified using TriZol® reagent (Invitrogen, Carlsbad, CA, USA). RNA integrity was verified by 1.5% agarose gel electrophoresis and 260/280 absorbance ratio. RNA was treated with DNase I (Ambion Inc., Austin, TX, USA) before cDNA synthesis, to avoid DNA contamination. One microgram of total RNA was used to prepare cDNA. cDNA synthesis was performed using the Verso cDNA Synthesis Kit (Thermo Scientific, US) according to the manufacturer's instructions in the G Palm Thermal Cycler (Model PTC-200, Watertown, MA, USA).

4.2.15 Relative gene expression analysis

First strand cDNA was used as a template with gene-specific primers to synthesize second strand DNA by conventional PCR. Expression kinetics of *IL1R1*, *IL1RN*, *IL1A*, *IL1B*, *IL6, TNFA*, *ICAM1*, *MITF-M*, *IL8*, *TYR* and *TYRP1* genes were analysed. Glyceraldehyde 3-phosphate dehydrogenase (*GAPDH)* was used as internal control (Table 2). Reactions were performed according to the manufacturer's instructions (Fermentas, Burlington, ON, Canada). DNA fragments were amplified for 39 cycles and signal intensities were analysed on 3.5% agarose gel stained with ethidium bromide. Densitometric analysis was performed using Alpha Imager software, and mean density for respective genes with respect to *GAPDH*, was plotted.

Table 2: Primer sequences used for gene expression analysis.

Primer	**Sequence (5' to 3')**	**Amplicon size (bp)**	**Annealing Temperature (^{0}C)**
IL1R1 FP	GGAGGCTGATAAATGCAAGG	195	62
IL1R1 RP	GTAAGATGAATTTACCACGC		
IL1RN FP	GCTGGAGGCAGTTAACATC	165	65
IL1RN RP	CTACTCGTCCTCCTGGAAG		
IL1A FP	GCTGCTGAAGGAGATGCCTG	143	66

IL1A RP	CTACGCCTGGTTTTCCAGT		
IL1B FP	AGATGAAGTGCTCCTTCCAGG	153	65
IL1B RP	TGGTCGGAGATTCGTAGCTG		
IL6 FP	AAATTCGGTACATCCTCGACGGCA	88	62
IL6 RP	AGTGCCTCTTTGCTGCTTTCACAC		
TNFA FP	GCCCCCAGAGGGAAGAGTTCCCCA	124	70
TNFA RP	GCTTGAGGGTTTGCTACAACATGGGC		
ICAM1FP	TCTGTTCCCAGGACCTGGCAATG	282	65
ICAM1RP	GGAGTCCAGTACACGGTGAGGAAG		
MITFM FP	CAAATGATCCAGACATGCGCTGG	180	61
MITFM RP	CTCGAGCCTGCATTTCAAGTTCC		
IL8FP	GATCCACAAGTCCTTGTTCCA	110	56
IL8RP	GCTTCCACATGTCCTCACAA		
TYRFP	AGCACCCCACAAATCCTAACTTAC	92	63
TYRRP	ATGGCTGTTGTACTCCTCCAATC		
TYRP1FP	TTTGTAACAGCACCGAGGATG	192	62
TYRP1RP	TGGGGTCACTGTAACCTTCCAC		
GAPDH FP	CATCACCATCTTCCAGGAGCGAG	122	65
GAPDH RP	CCTGCAAATGAGCCCCAGCCT		

4.2.16 Statistical analyses

All the experiments were performed at least three times in triplicates independently using different batches of cells. Data are presented as the mean ± standard deviation (SD) and the statistical difference between two groups was analyzed by Student's t-test using GraphPad Prism version 3.02 software (GraphPad Software Inc. San Diego, CA, USA). *p*-values less than 0.05 were considered statistically significant. Histopathological studies: for measuring the epidermal thickness was performed using the Image J software (Stat Soft, Inc., USA). Descriptive statistics of quantitative traits was presented as mean. The Correlation between the length of epidermal thickness between patients and control was analyzed in GraphPad Prism version 3.00 for Windows (GraphPad Software, San Diego California, USA) where unpaired t-test was used for comparison of unrelated groups between NL, PL, L compared to control. In testing hypotheses, the differences were considered statistically significant at $p < 0.05$.

4.3 RESULTS

4.3.1 Histopathological analysis of skin biopsies (A) Viable epidermal thickness and rete-ridges pattern:

To examine the difference in skin architecture of vitiligo patients and controls, Hematoxylin and Eosin (H&E) staining was performed to assess epidermal hyperplasia/ epidermal thickening, viable epidermis thickness and the pattern of rete-ridges in skin biopsies derived from lesional (L), peri-lesional (PL), non-lesional (NL) and healthy matched controls. Our results showed significant increase in viable epidermal thickness in lesional compared to control (p=0.0100) as well as in non-lesional compared to lesional skin (p=0.0304) (Figure 1). Also, significant increase in the epidermal thickness between control and lesional skin was observed (p=0.0082). Similarly, significant difference in epidermal thickness between non-lesional and lesional skin was observed (p = 0.0442).

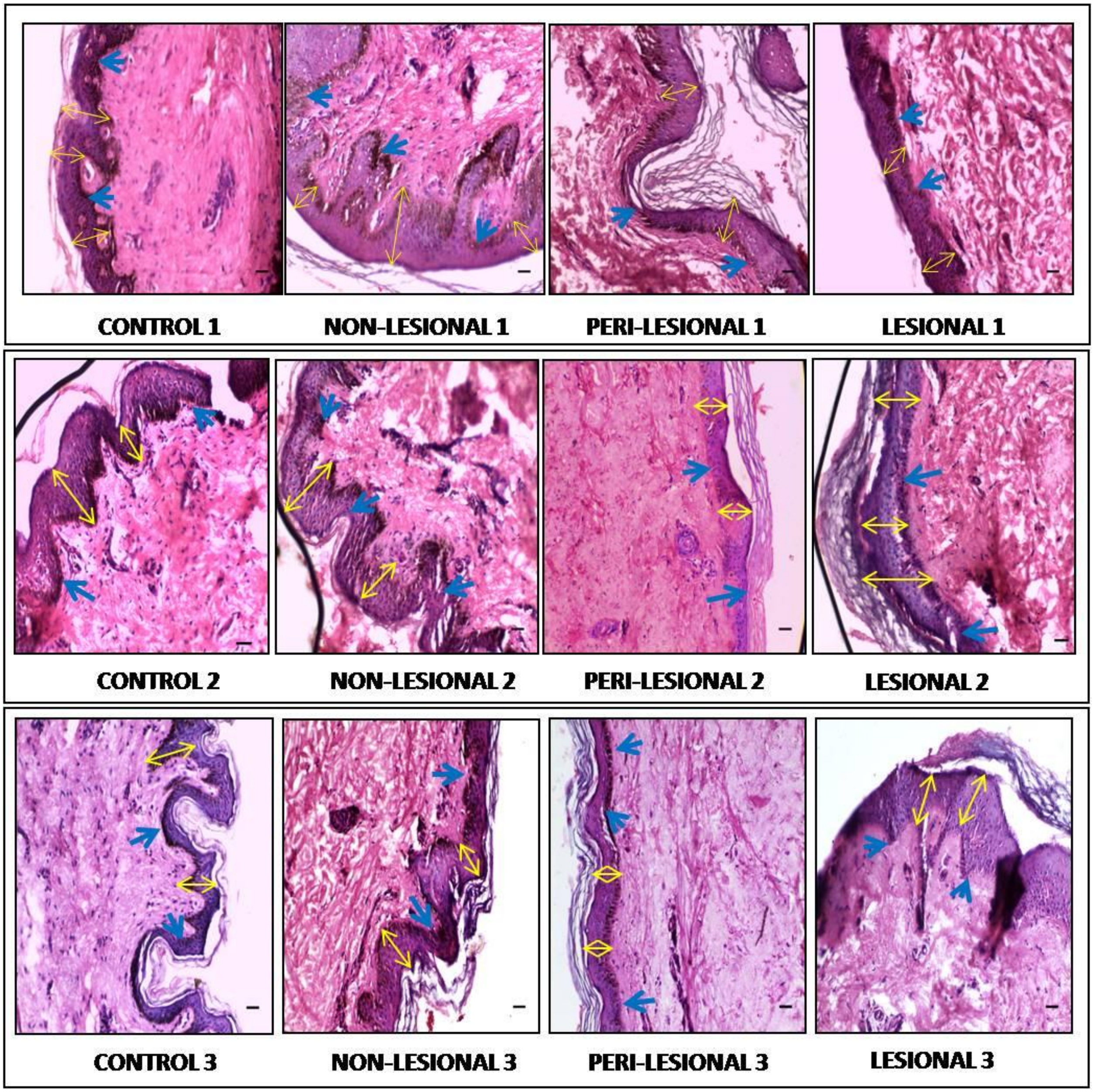
CONTROL 1
NON-LESIONAL 1
PERI-LESIONAL 1
LESIONAL 1
CONTROL 2
NON-LESIONAL 2
PERI-LESIONAL 2
LESIONAL 2
CONTROL 3
NON-LESIONAL 3
PERI-LESIONAL 3
LESIONAL 3

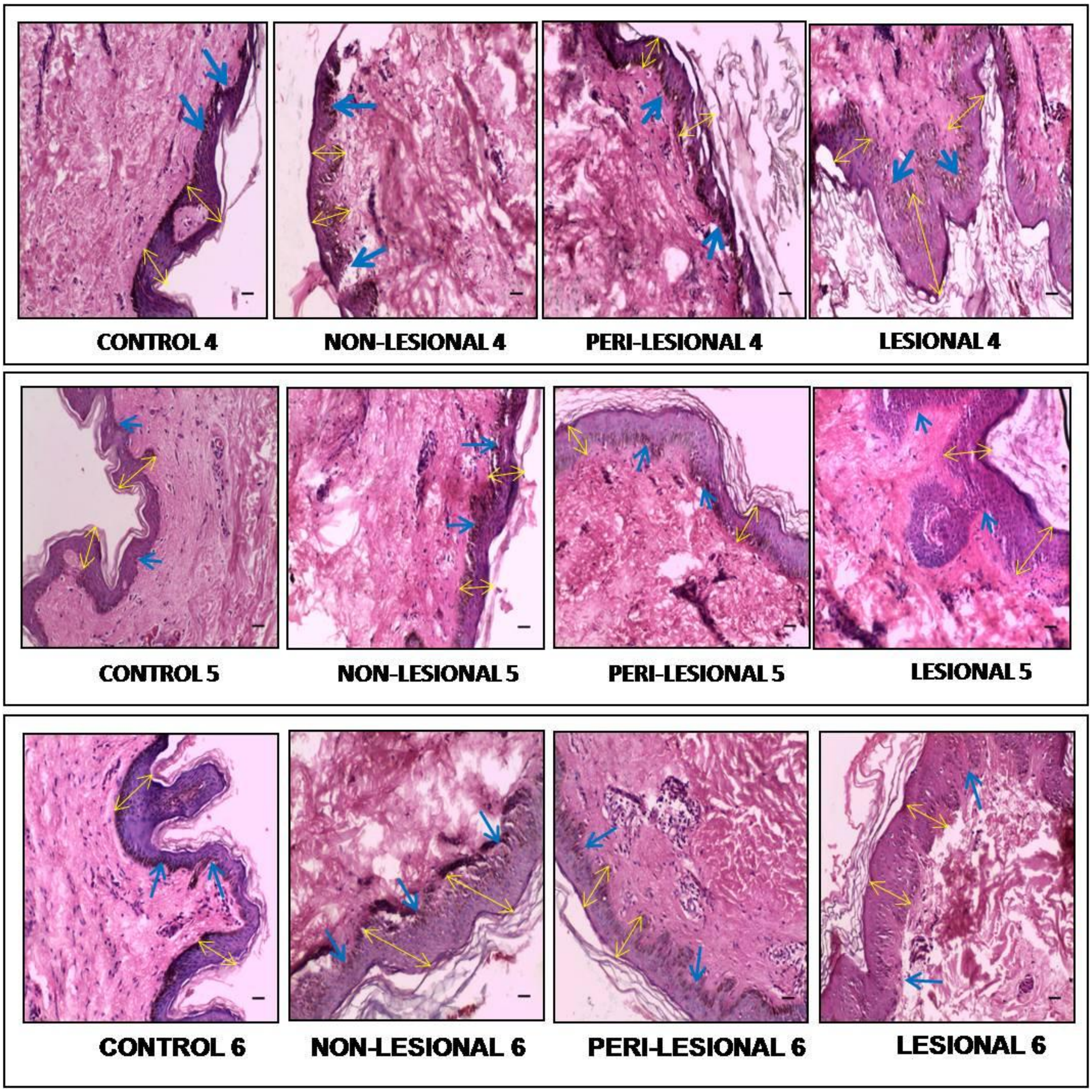

Figure 1: H & E stained tissue samples from vitiligo patients and healthy controls: Change in length of viable epidermis and pattern of rete-ridges was observed at magnification 20X. Yellow arrows represent epidermal thickness (µm); blue arrows represent the pattern of rete-ridges between vitiligenous skin and control skin (n=6). Scale: 10µm.

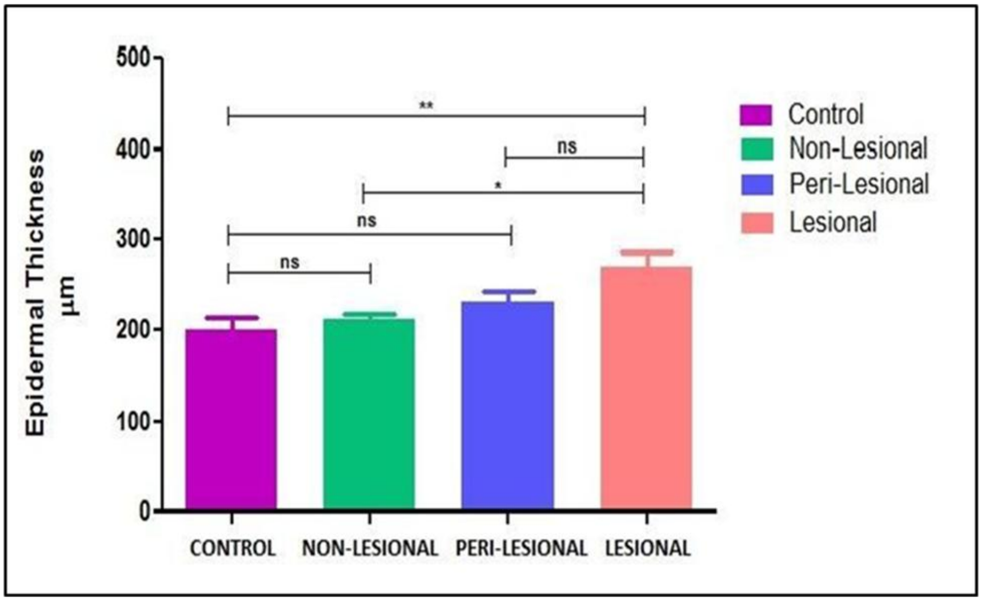

Figure 2: Viable epidermal thickness: Significant increase in viable epidermal thickness was observed in lesional (L) compared to control (*p* =0.0100) as well as in non-lesional compared to lesional (*p*=0.0304) skin.

(B) MITF-M expression in skin biopsies of control and vitiligo patients: In order to observe the expression levels of MITF-M in skin biopsies of vitiligo patients and controls, we performed immunofluorescence studies (Figure 3). Our results showed decreased levels of MITF-M in lesional and non-lesional skin of vitiligo patients as compared to controls (*p*=0.0282 and *p*=0.0039 respectively) (Figure 4; n=3).

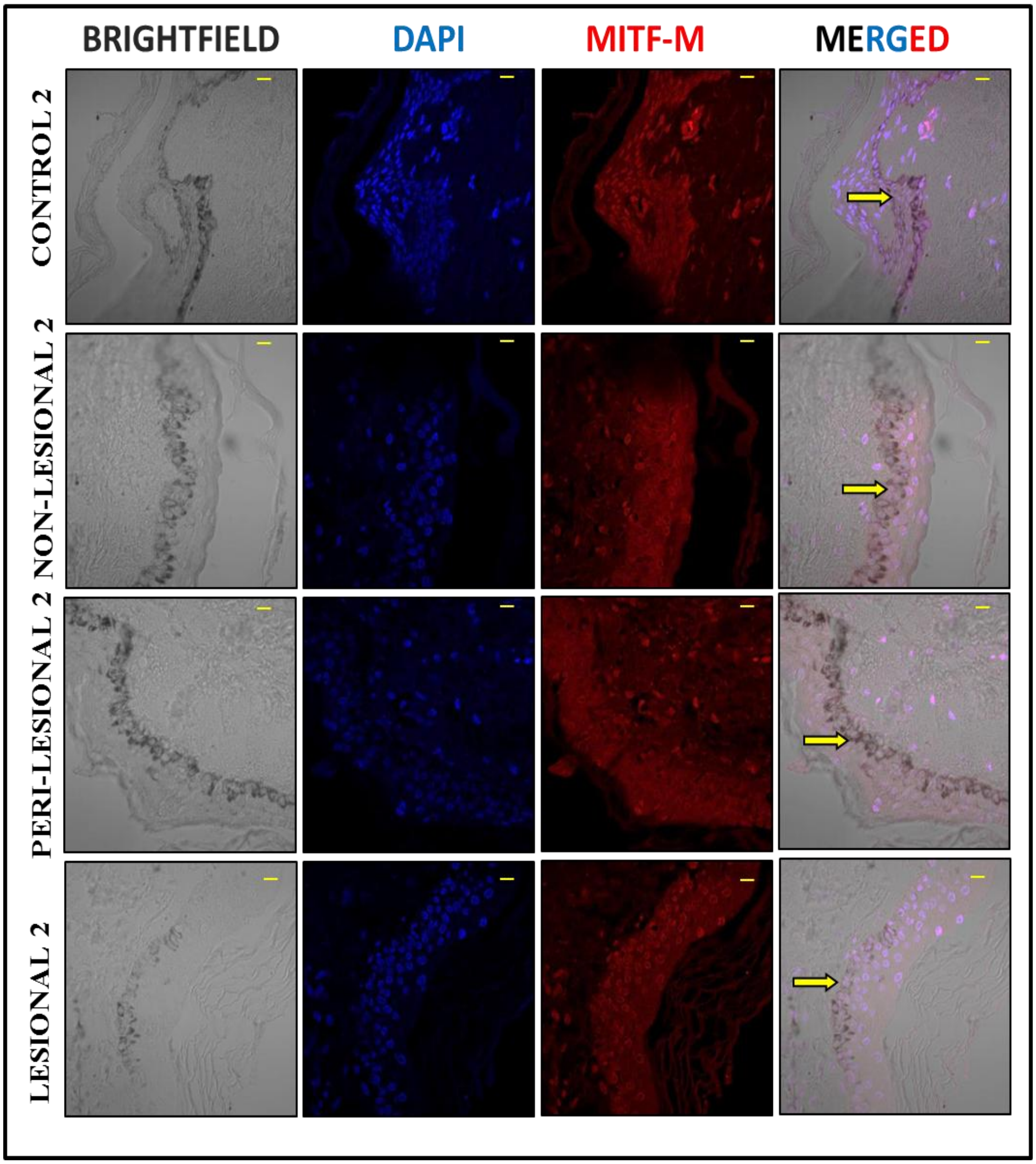

Figure 3: MITF-M expression in control, lesional, non-lesional and peri-lesional skin by Immunofluorescence (Magnification: 63 X; Scale: 100 μm).

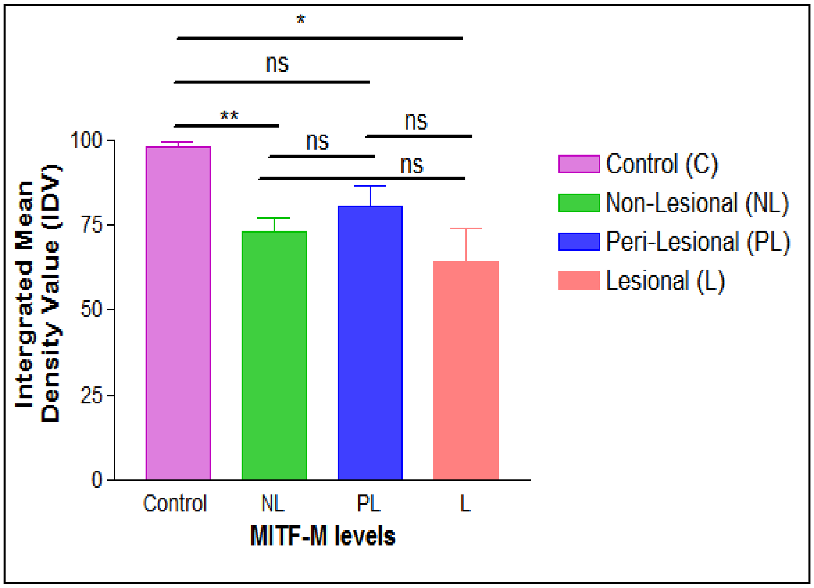

Figure 4: Densitometric analysis of *in situ* MITF-M levels monitored by immunofluorescence: MITF-M levels were found to be significantly decreased in NL vs. C skin (p= 0.0039) and L vs. C skin (p= 0.0282; n=3).

4.3.2 Effect of TNF-α on melanocyte biology:

4.3.2.1 Dose dependent effect of TNF-α on melanocyte cell death:

Primary melanocytes were treated with different doses of TNF-α (0, 10, 50, 100 ng/ml) for 24 and 48 hrs (n=3). No significant difference was observed in morphology and cell death up to 24 hrs (data not shown). However, after 48 hrs of treatment, there was a significant increase in cell death of melanocytes in a dose dependent manner of TNF-α treatment (10, 20, 50 and 100 ng/ml) (Figure 5A and B; p<0.005).

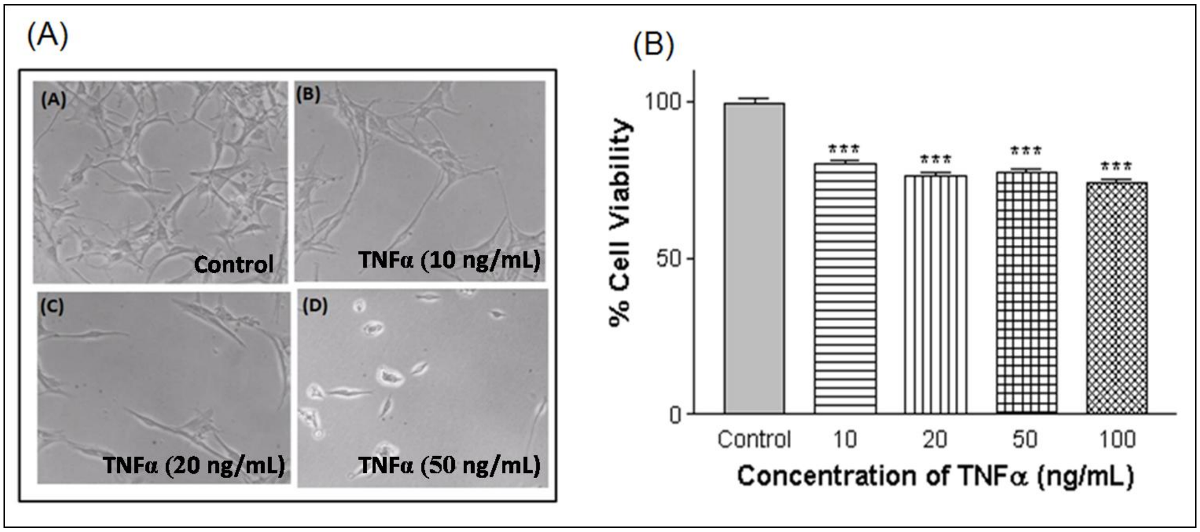

Figure 5: Effect of TNF-α on NHM death: (A) Morphological observation of the effect of TNF-α treatment (a) Control b) 10 ng/ml c) 20 ng/ml d) 50 ng/ml) on NHM as compared to untreated cells (Magnification: 10X; Scale 100μm). (B) Dose dependent effect of exogenous stimulation by TNF-α on melanocytes (0-100 ng/ml TNF-α, 48 hrs).

4.3.2.2 Effect of TNF-α on cellular ROS:

For further experiments, 10ng/ml and 48 hrs of TNF-α dose were selected as it is the minimum concentration with significant effect on the melanocyte viability. We found significant increase in the cellular ROS levels (p=0.0290; n=4; Figures 6A and 6B) in NHM upon TNF-α treatment as compared to untreated cells.

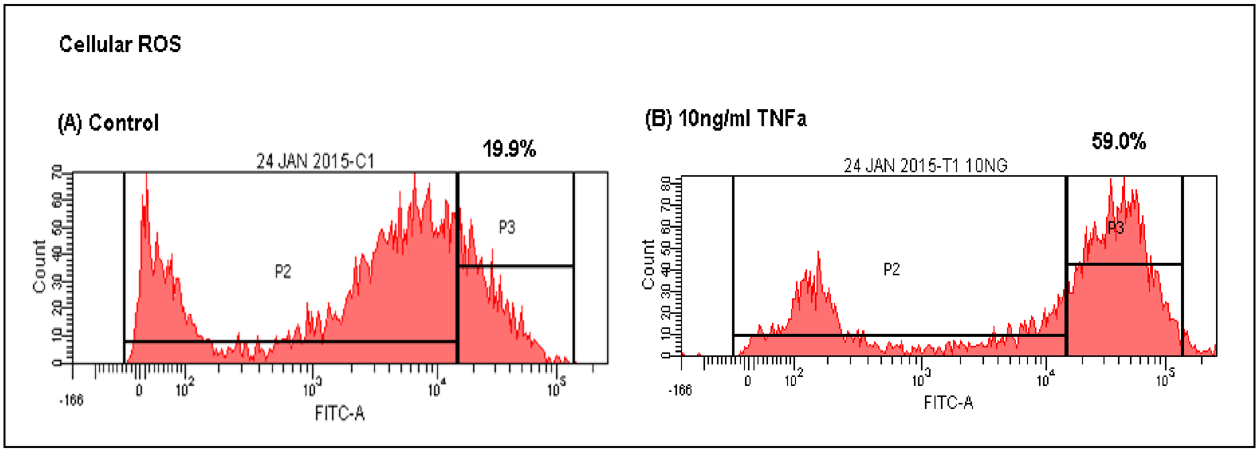

Figure 6: Estimation of cellular ROS levels at 10 ng/ml TNF-α at 48 hrs in NHM. Analysis of ROS levels by FACS in NHM treated with TNF-α and control revealed significant increase in ROS levels upon TNF-α treated treatment (n=4).

4.3.2.3 Effect of TNF-α on mitochondrial ROS:

Further, we monitored the effect of TNF-α on mitochondrial ROS levels and found significant increase in mitochondrial ROS levels (*p*=0.0033; n=3; Figures 7A and 7B) in NHM upon TNF-α treatment as compared to untreated cells.

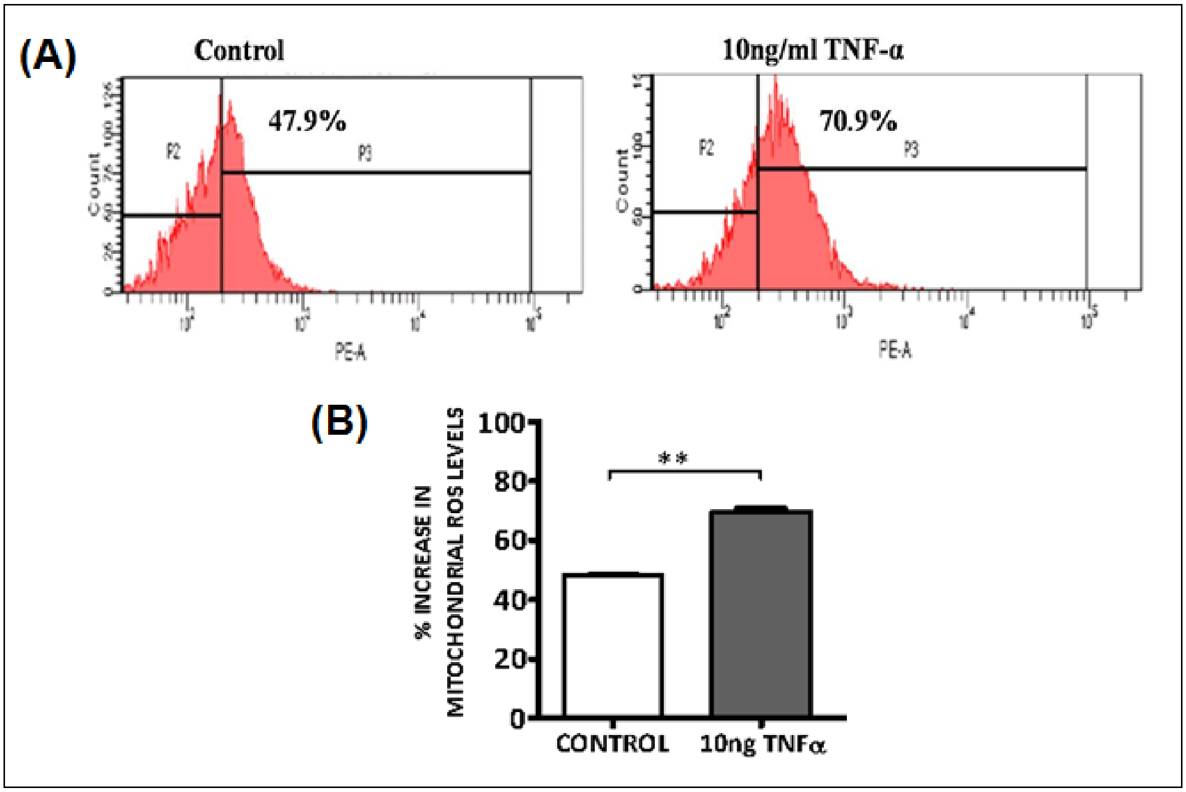

Figure 7: Analysis of Mitochondrial ROS levels in TNF-α treated as compared to untreated NHM: (A) Analysis of mitochondrial ROS levels by FACS in NHM treated with TNF-α and control. (B) Significant increase was found in mitochondrial ROS at 10 ng/ml TNF-α compared to control (48 hrs; *p*=0.0033; n=3).

4.3.2.4 Effect of TNF-α on Complex 1 activity:

In the electron transport chain (ETC), complex 1 is one of the major sites of mitochondrial ROS generation; therefore we aimed to monitor the complex 1 activity in TNF-α treated NHM as compared to untreated cells. Interestingly, we found ~20% decrease in complex 1 activity in TNF-α treated NHM compared to untreated NHM.

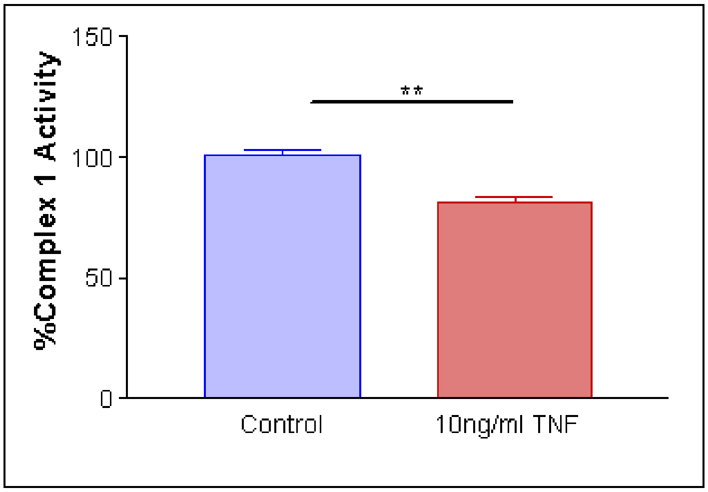

Figure 8: Effect of TNF-α on Complex 1 activity: Complex 1 analysis showed ~20% decrease in complex 1 activity upon TNF-α treatment as compared to controls (48 hrs; n=3).

4.3.2.5 Effect of TNF-α stimulation on AIF expression in NHM:

As we found increased mitochondrial ROS levels with concomitant decrease in complex 1 activity, we monitored the effect of TNF-α on AIF levels. It has been suggested that AIF plays a vital role in mitochondrial respiration and redox metabolism. AIF may interact with complex I and complex III of ETC and helps in structural maintenance (Sevrioukova, 2011). However, our results showed no significant difference in AIF levels upon TNF-α treatment.

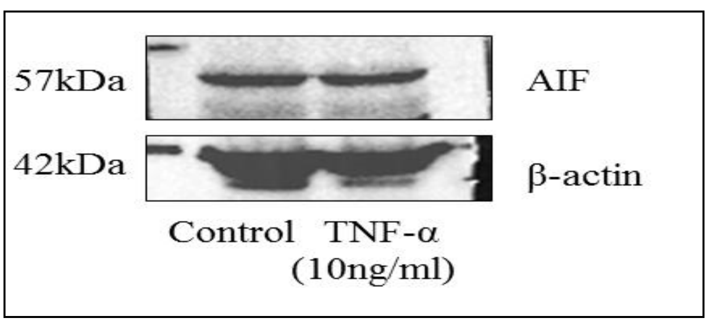

Figure 9: Effect of TNF-α on AIF levels: No significant difference was observed in AIF levels after 48 hrs of TNF-α treatment to NHM as compared to untreated cells (n=3).

4.3.2.6 Effect of TNF-α on Melanogenesis and *IL6* and *ICAM1* expression: NHM were treated with 10ng/ml TNF-α for 48 hrs and analyzed for transcript levels of melanin synthesis genes (*MITF-M, TYR*) melanin content along with *IL6* and *ICAM1* expression levels. Our results showed significant decrease in the expression of melanin synthesis genes *MITF-M* and *TYR* (p=0.0055 and p=0.0055 respectively) with concomitant decrease in melanin content (Figure 10. A, B and C). Moreover, TNF-α treatment resulted in significant increase in the expression of *IL6* as well as *ICAM1* (p=0.0044 and p=0.0072 respectively) (Figures 10. D and E). Furthermore, we demonstrated significant decrease in the protein expression of MITF-M upon 10ng/ml TNF-α treatment on NHM for 48 hrs (Figure 11; p=0.0004; n=3).

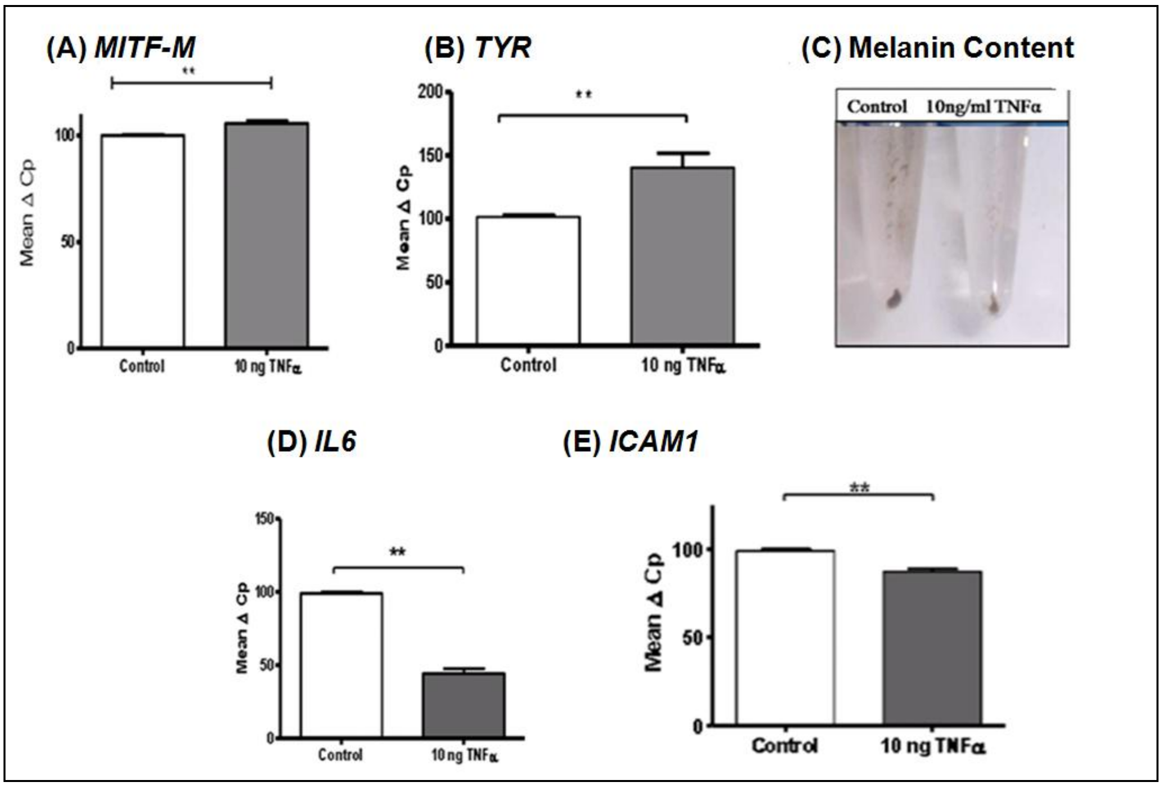

Figure 10: Effect of TNF-α on melanogenesis and, *IL6* and *ICAM1* expression: Exogenous stimulation of TNF-α (10 ng/ml; 48 hrs) on NHM caused (A) significant decrease in *MITF-M* levels (p=0.0055), (B) significant decrease in *TYR* levels (p=0.0055) and (C) significant decrease in Melanin content whereas (D) significant increase in *IL6*

(*p*=0.0044) and (E) significant increase in *ICAM1* levels (*p*=0.0072) were observed in NHM upon TNF-α stimulation (n = 3).

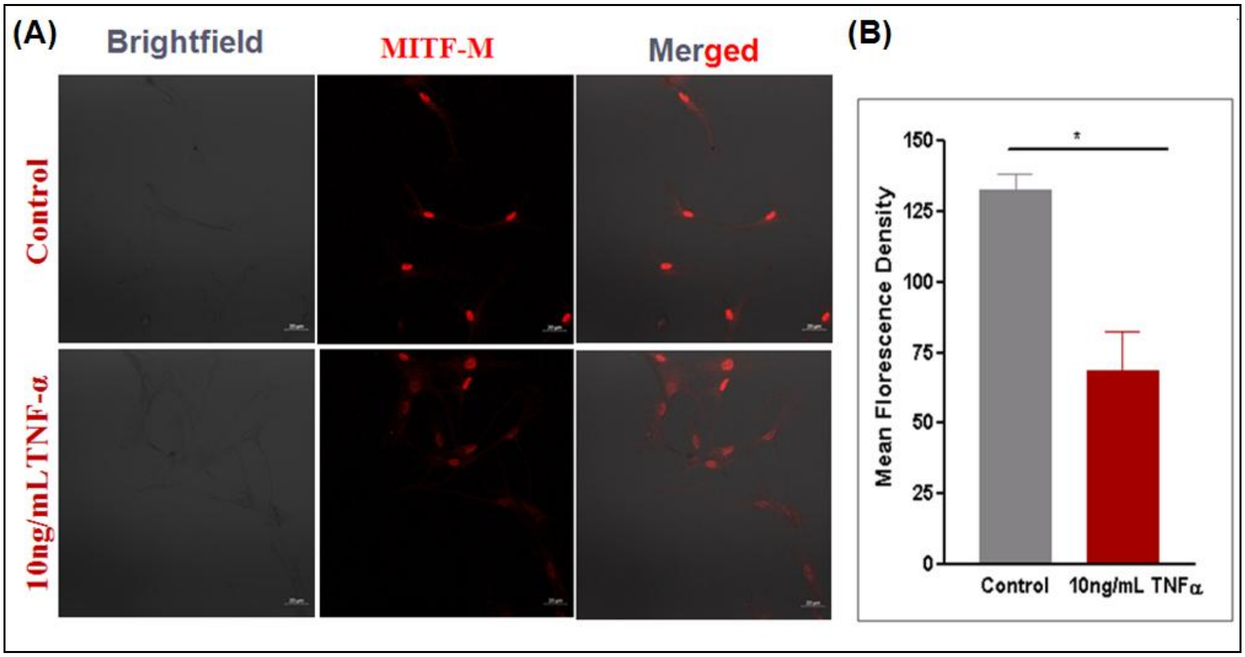

Figure 11: Analysis of MITF-M expression by Immunofluorescence upon exogenous stimulation of TNF-α (10ng/ml; 48hrs) on NHM: (A) MITF-M expression analysis by confocal microscopy at (Magnification: 63X; Scale 20μm) (B) Mean fluorescence densitometric analysis showed significant reduction in the expression of MITF-M in TNF-α induced NHM compared to control (*p*=0.0004; n=3).

4.3.2.7 Effect of TNF-α on Autophagy induction: NHM were treated with TNF-α in a time dependent manner for 12hrs, 24hrs and 48 hrs and observed for autophagy induction by LC3-I to LC3-II conversion. Our results showed induction of autophagy in NHM around 12 hrs of treatment which was confirmed by LC3-I to LC3-II conversion whereas at 24 and 48 hrs, no significant difference was observed for LC3-I to LC3-II conversion.

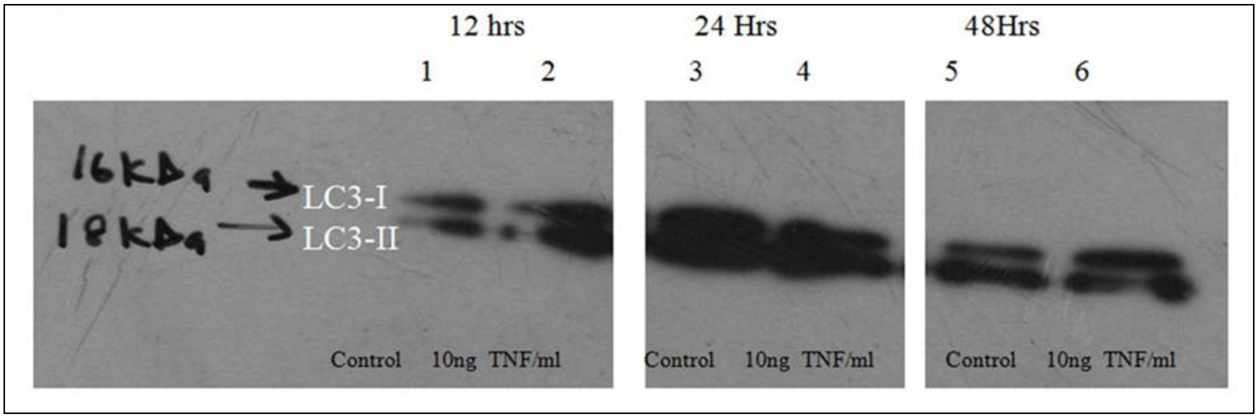

Figure 12: Effect of TNF-α on Autophagy induction: Exogenous stimulation of TNF-α (10ng/ml; 48 hrs) induced autophagy in NHM around 12 hrs of treatment which was confirmed by western blot analysis of LC3-I to LC3-II conversion, whereas at 24 and 48 hrs, no significant difference was observed for LC3-I to LC3-II conversion.

4.3.2.8 Effect of TNF-α on NHM Apoptosis:

In order to elucidate the mode of cell death mediated by TNF-α, we have monitored caspase 8 cleavage. TNF-α binds to cell surface receptors and in turn induces the activation and cleavage of the initiator procaspase 8. After 48 hrs of TNF-α treatment, we observed 18 kDa and 42 kDa cleaved fragments of procaspase 8. NF-κB has been reported to be involved in downstream signaling of various inflammatory and cell death pathways. However, we did not find any significant difference for NF-κB p65 levels in TNF-α treated NHM as compared to untreated NHM.

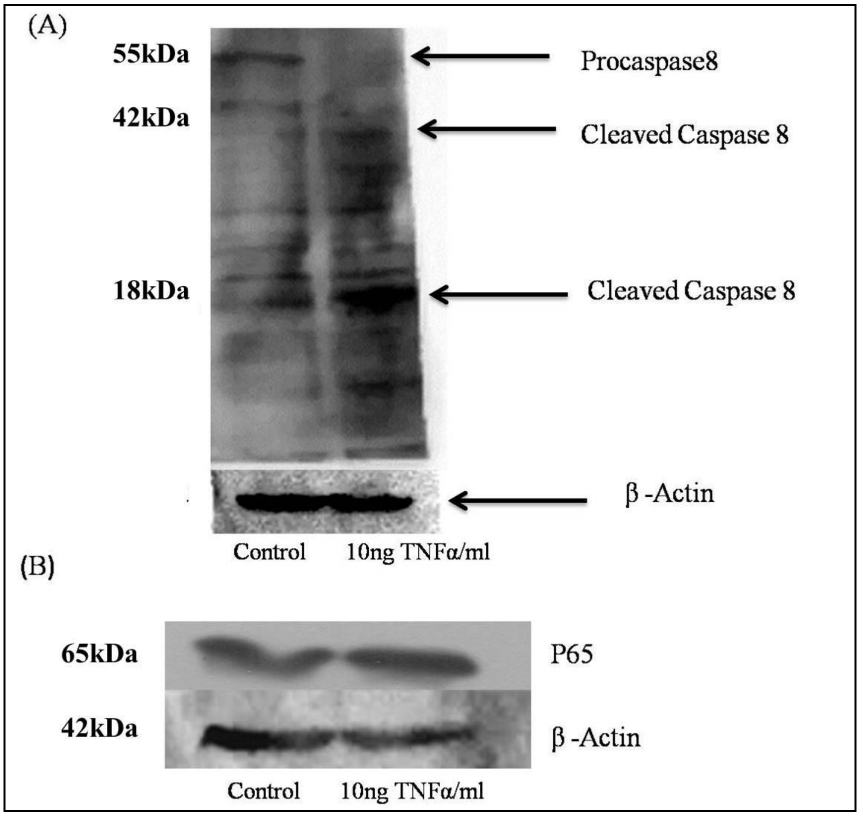

Figure 13: Effect of TNF-α on apoptosis of NHM by western blot: (A) TNF-α (10 ng/ml; 48 hrs) induced apoptotic cell death evidenced by caspase 8 cleavage (B) No difference was observed in the NF-κB p65 levels post TNF-α treatment (n=3).

4.3.3 Role of IL-6 in melanocyte biology:

4.3.3.1 Dose dependent effect of IL-6 on melanocyte cell death:

Primary melanocytes were treated with IL-6 in a dose dependent manner (0, 10, 50, 100 ng/ml) for 24 hrs and 48 hrs (n=3). No significant difference was observed in the cell morphology and cell death up to 24 hrs (data not shown). However, after 48 hrs of treatment, there was a significant increase in cell death in a dose dependent manner of IL-6 treatment (10, 20, 50 and 100 ng/ml) (Figure 14 A and B; $p<0.005$).

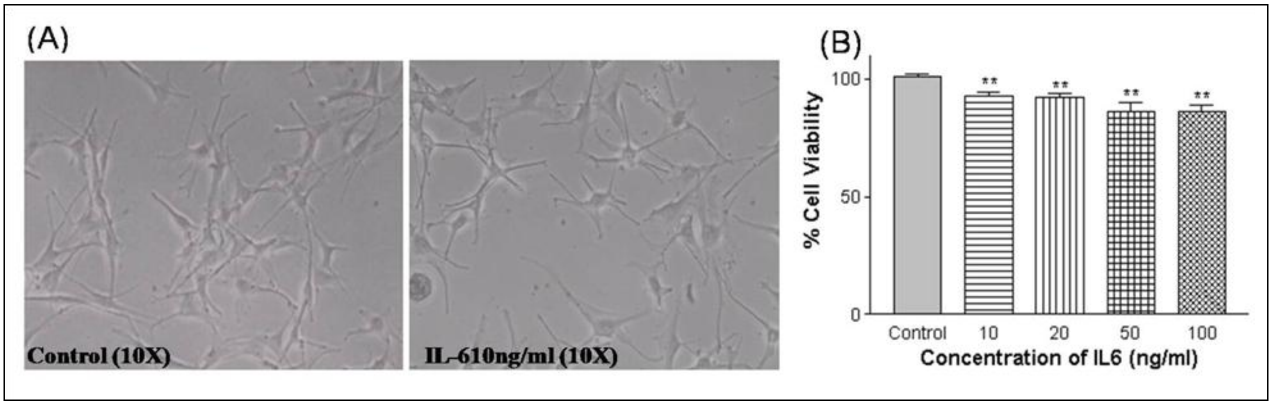

Figure 14: Effect of IL-6 on melanocyte cell death: (A) No morphological effect of IL-6 was found on the proliferation of NHM as compared to untreated NHM (Magnification: 10X Scale:100μm. (B) Significant increase in cell death of melanocytes was observed upon exogenous stimulation of IL-6 in a dose dependent manner (0-100 ng/ml IL-6, 48 hrs) (n=3).

4.3.3.2 Effect of IL-6 on *MITF-M*, *TYR* and *ICAM1* transcript levels in NHM:

Exogenous stimulation by IL-6 (50 ng/ml; 48 hrs) on NHM showed significant decrease in *MITF-M* expression in a dose dependent manner (10, 20 and 50 ng/ml; 48 hrs) upon IL-6 treatment (p= 0.0332; p=0.0117 and p=0.0050 respectively) (Figure 15 A). However, *TYR* expression was unaffected at 10 and 20 ng/ml of IL6 for 48 hrs while higher concentration (50 ng/ml; 48 hrs) resulted in a significant down regulation of *TYR* expression (p=0.0465; Figure 15 B). *ICAM1* was up regulated by IL6 at 20 and 50 ng/ml; 48 hrs treatment (p=0.0276 and p=0.0170 respectively); whereas at 10 ng/ml IL6 treatment for 48 hrs there was no difference in *ICAM1* expression (p=0.2487; Figure 15 C).

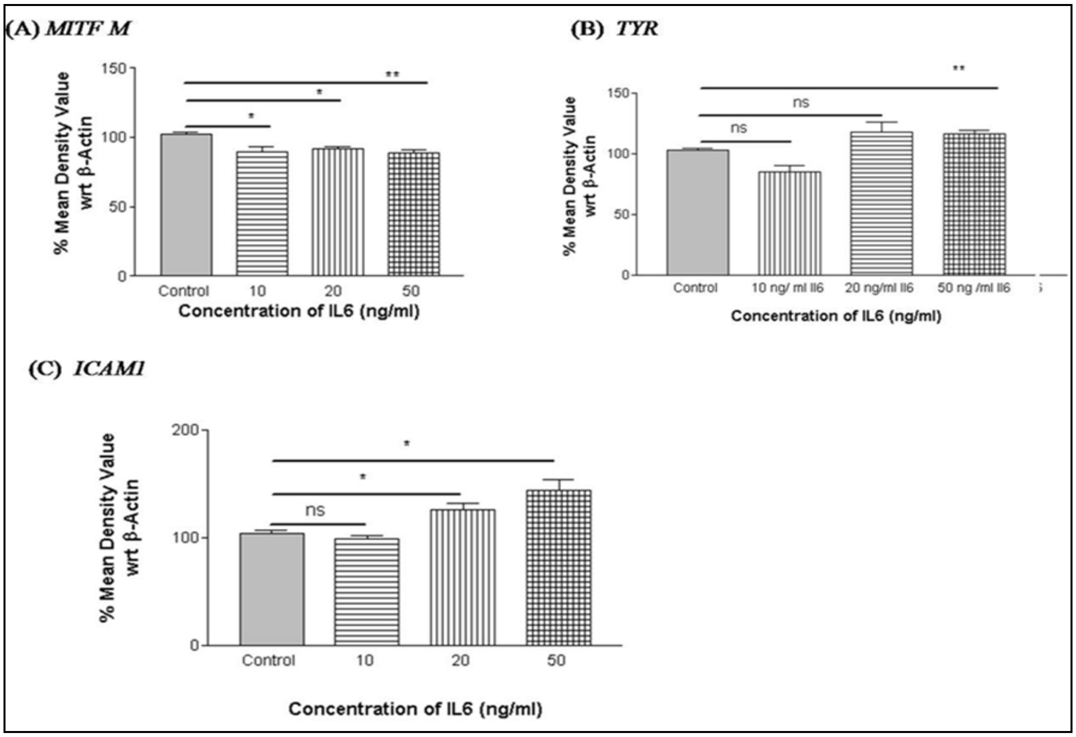

Figure 15: Effect of IL-6 on *MITF-M, IL6R* and *ICAM1* expression in NHM: Semi quantitative relative gene expression of *MITF M*, *TYR*, *IL6R* and *ICAM1* genes upon 10, 20 and 50 ng/ml IL-6 stimulation in NHM, with respect to *GAPDH* as a reference gene. (A) Significant decrease in *MITF-M* was observed in a dose dependent manner (10, 20 and 50ng/ml; 48hrs) upon IL-6 treatment (*p*= 0.0332; *p*=0.0117 and *p*=0.0050 respectively). (B) 50 ng/ml IL-6 at 48 hrs resulted in significant down regulation of *TYR* expression (*p*=0.0465). However, no significant difference was seen in *IL6*R transcript levels at the lower concentration of IL-6. (C) *ICAM1* was up regulated by IL-6 (20 and 50 ng/ml; 48 hrs) treatment (*p*=0.0276 and *p*=0.0170) respectively whereas at 10 ng/ml IL-6 treatment (48 hrs) caused no difference in *ICAM1* expression (*p*=0.2487). All the experiments were performed in triplicate and means ± S.D. have been shown in figures [**p*<0.05, ***p*<0.01, ****p*<0.001, *p*>0.05, ns (non significant)].

4.3.3.3 Effect of IL-6 on MITF-M expression: As we observed decreased transcript levels of *MITF-M* upon Il-6 treatment, we were further interested to monitor the effect of IL-6 on protein expression of MITF-M on NHM. However, our results showed no significant difference in MITF-M protein expression in NHM (p = 0.2258; n=3).

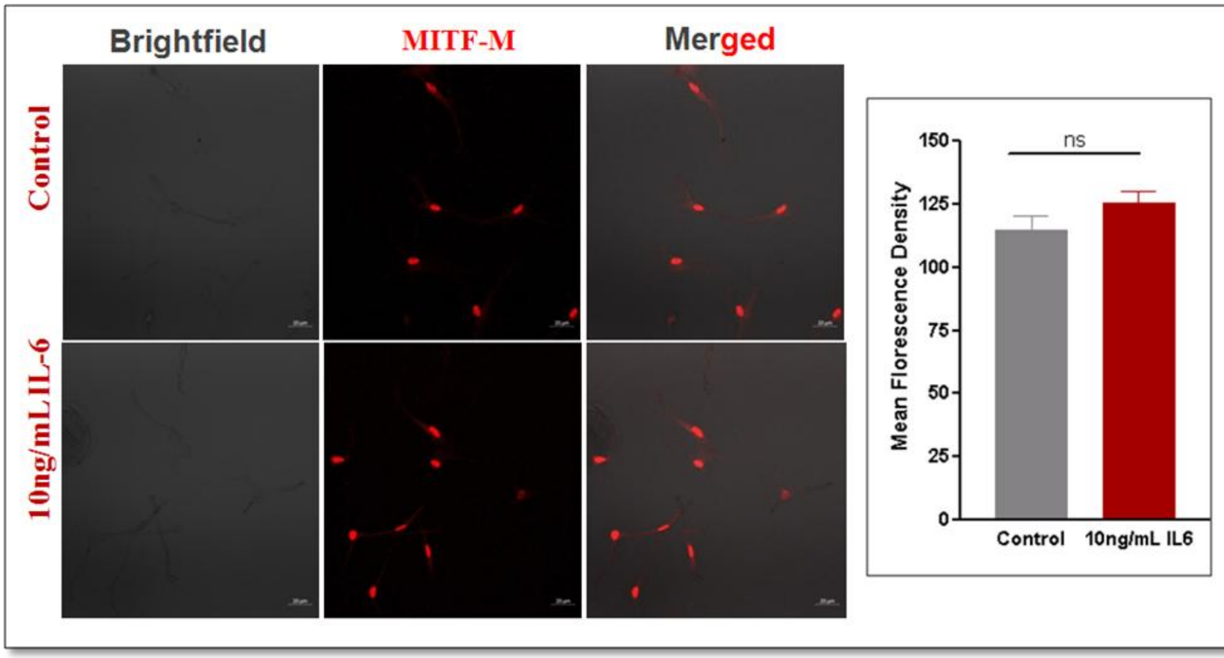

Figure 16: Analysis of MITF-M levels in NHM upon IL-6 treatment by Immunofluorescence: Treatment with IL-6 (10 ng/mL) did not cause any significant change in MITF-M protein expression levels. (n=3; treatment duration 48 hrs; Magnification 63X: scale bar 20µ; p=0.2258).

4.3.4 Role of IL-1α on melanocyte biology:

4.3.4.1 Dose dependent effect of IL-1α on melanocytes cell death:

Primary melanocytes were treated with the different doses of IL-1α (0, 10, 50, 100 ng/ml) and observed after 24 and 48 hrs for the cell morphology and viability (n=3). The NHM did not show any difference in morphology and viability up to 24 hrs (data not shown). Also, there was no significant morphological change observed in NHM even after 48 hrs of IL-1α treatment (Figure 17 A). However, 100 ng/ml of IL-1α treated NHM showed significant decrease in cell viability (p=0.0210) after 48 hrs of treatment, as compared to untreated NHM (Figure 17 B). However, 10 & 50 ng/ml doses of IL-1α did not show any significant difference (p=0.6658 and p=0.9301 respectively) in cell viability.

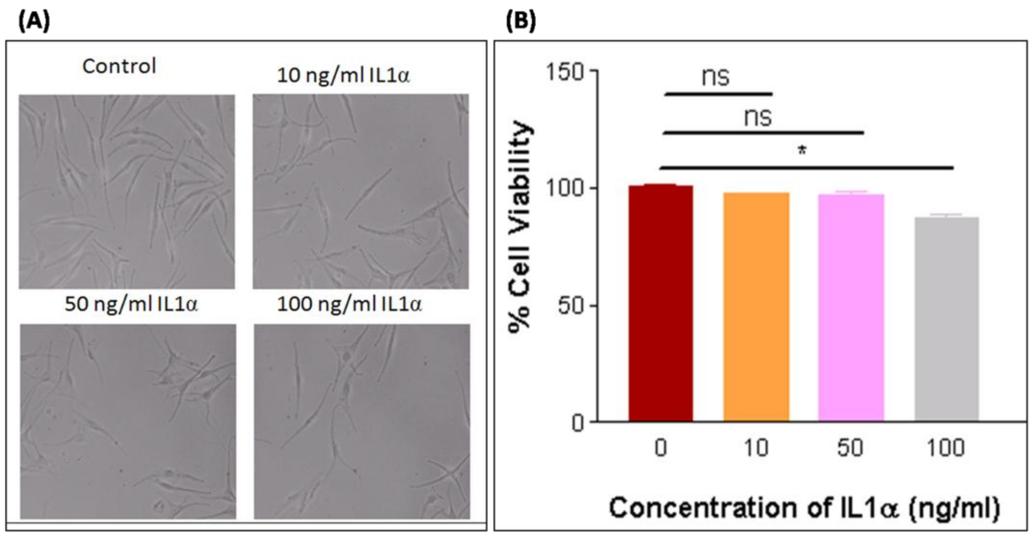

Figure 17: Dose dependent effect of exogenous stimulation of IL-1α on melanocytes cell death (0-100 ng/ml IL-1α, 48 hrs): (A) NHM showed no cell morphological changes after 48 hrs of IL-1α treatment (Magnification: 10X; Scale: 100µm). (B) Mean % cell viability on 100 ng/ml IL-1α treatment showed significant decrease in cell viability after 48 hrs (n=3, $p<0.0210$). However, 10 & 50 ng/ml doses of IL-1α did not show any significant difference in cell viability.

4.3.4.2 IL-1α regulates melanogenesis and other immunomodulatory genes:

IL-1α (10 and 100 ng/ml) treated NHM were used for expression analysis of *IL1RN*, *IL1A*, *IL1B*, *IL6*, *TNFA*, *ICAM1*, *MITF-M*, *IL8*, *TYR* and *TYRP1* genes. Our results showed significant decrease in expression of *MITF-M* in 100 ng/ml IL-1α treated NHM as compared to untreated NHM ($p=0.0066$; Fig. 18). However, there was no difference at 10 ng/ml IL-1α treatment ($p=0.0694$). Also, *TYR* and *TYRP1* genes of melanin synthesis pathway exhibited no significant difference ($p=0.4532$, $p=0.5659$; $p=0.4395$, $p=0.8858$) upon IL-1α treatment (10 and 100 ng/ml respectively). Interestingly, the expression levels of *IL1RN, IL1A, IL1B, IL6, TNFA* and *ICAM1* were significantly up regulated in 100 ng/ml IL-1α treated NHM as compared to untreated NHM ($p=0.0005$, $p=0.0063$, $p<0.0001$, $p<0.0001$, $p=0.0034$ and $p=0.0017$ respectively). Also, *IL1RN*, *IL1B*, *TNFA* and *ICAM1* were found to be significantly up regulated in 10 ng/ml IL-1α treated NHM as compared to untreated NHM ($p=0.0360$, $p=0.0385$, $p=0.0007$, and $p=0.0421$ respectively). However, no significant difference was observed for *IL1A* and *IL6* in 10 ng/ml IL-1α treated NHM as compared to untreated NHM (*p*=0.9001 and *p*=0.0841 respectively).While, transcript levels of *IL8* remained unaltered upon 10 ng/ml IL-1α (*p*=0.6838,) as well as 100 ng/ml IL-1α stimulation (*p*=0.7091; Fig. 18).

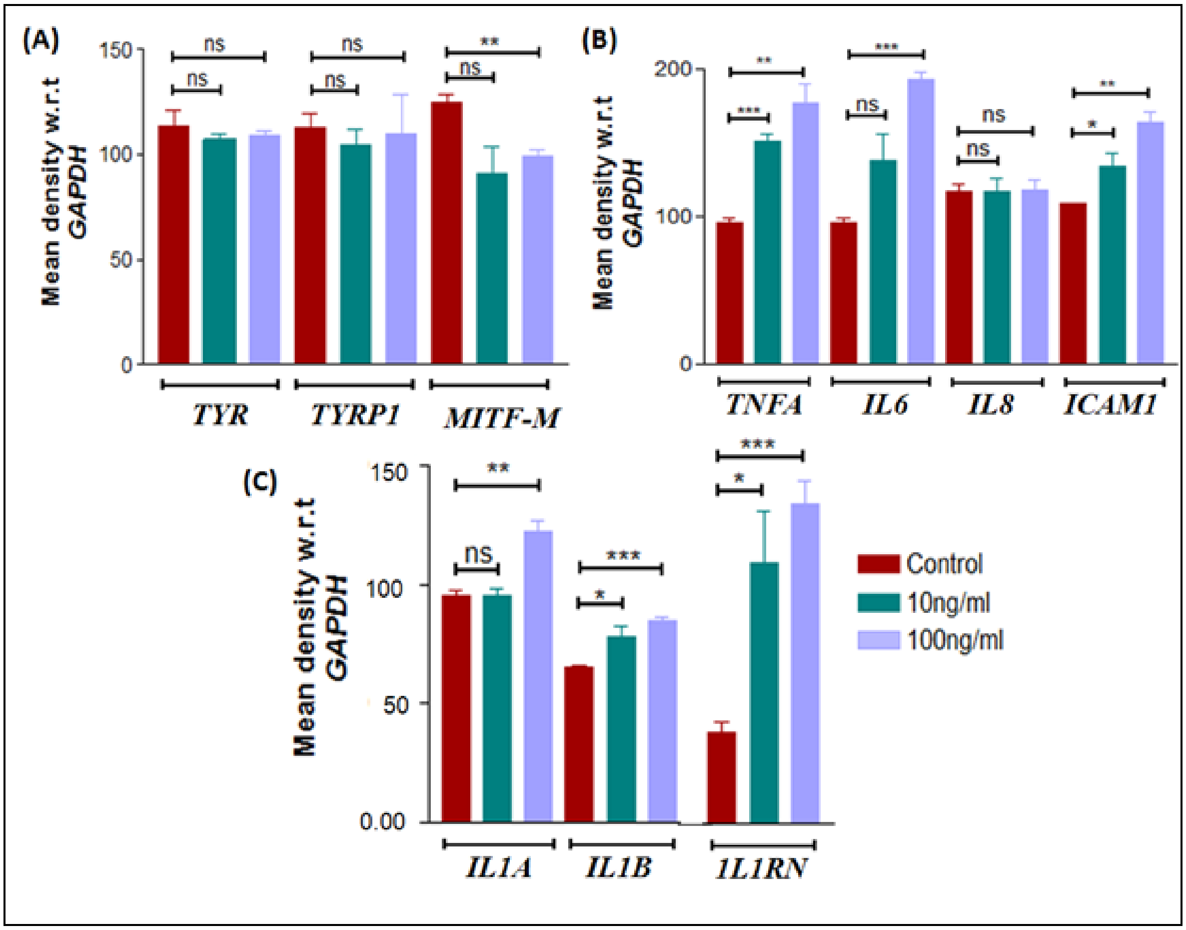

Figure 18: Effect of IL-1α on the genes involved in melanogenesis and other immuno-modulatory molecules in NHM. Semi quantitative relative gene expression analysis of *IL1RN, IL1A, IL1B, IL6, TNFA, ICAM1, MITF-M, IL8, TYR, TYRP1* genes with respect to *GAPDH* in NHM upon stimulation with 10 and 100 ng/ml IL-1α. (A) 100 ng/ml of IL-1α stimulation on NHM showed a significant decrease in *MITF-M* expression (*p*=0.0066) as compared to untreated NHM. However, no significant difference was observed for *TYR* and *TYRP1* expression upon IL-1α treatment (*p*>0.05). (B) 100 ng/ml IL-1α stimulation to NHM showed a significant increase in *TNFA* (*p*=0.0034), *IL6* (*p*<0.0001), *ICAM1* (*p*=0.0017) as compared to untreated NHM. Also, *TNFA* and *ICAM1* showed significantly

increased expression upon 10 ng/ml IL-1α stimulation to NHM. However, there was no difference in expression of *IL8* upon 10 ng/ml and 100 ng/ml IL-1α stimulation to NHM (p=0.6838 and p=0.7091 respectively). (C) 100 ng/ml IL-1α treated NHM showed significant increase in *IL1A* (p=0.0063), *IL1B* (p<0.0001) and *IL1RN* (p=0.0005) expression. Also, *IL1B* (p=0.0385) and *IL1RN* (p=0.0360) transcripts showed significant increase upon 10 ng/ml IL-1α stimulation to NHM. All the experiments were performed in triplicate and mean ± S.D. was shown in figures [*p<0.05, **p<0.01, ***p<0.001, p>0.05, ns (non significant)].

4.3.4.3 Effect of IL-1α on MITF-M expression: As we observed decreased transcript levels of *MITF-M* upon IL-1α treatment, we were further interested to monitor its effect on MITF-M protein expression. However, our results showed no significant difference in MITF-M protein expression in NHM upon IL-1α treatment (p = 0.1476; n=3).

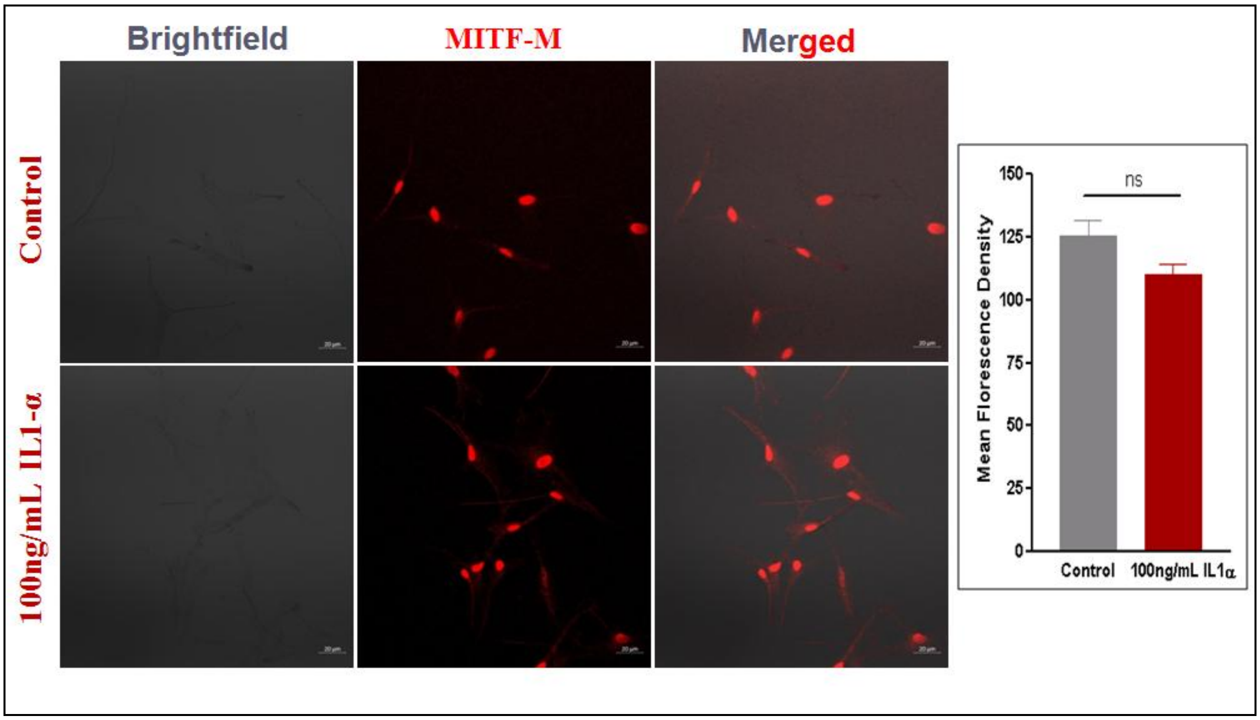

Figure 19: Analysis of MITF-M levels in NHM upon IL-1α treatment by Immunofluorescence: Treatment with IL-1α (100ng/mL) did not cause any significant change in MITF-M protein expression levels (treatment duration 48 hrs; scale bar 20µ; p = 0.1476; n=3).

4.3.5 Role of IL-10 in melanocyte biology:

4.3.5.1 Dose dependent effect of IL-10 on melanocyte cell death:

IL-10 did not show any significant effect on growth and viability of melanocytes in a dose dependent manner (0.25-100 ng/ml) (Figures 20 A and B). Further we have studied the effect of IL-10 on NHM (10ng/ml ;48 hrs) on melanin synthesis genes *MITF-M*, *TYR* and *ICAM-1*, and found no significant effect on *MITF-M* (p= 0.2401), *TYR* (p = 0.2934) and *ICAM1*(p=0.3608) transcript levels (n=3) (Figure 21). Interestingly, we observed significant increased expression of MITF-M protein levels on IL-10 (10ng/ml) treatment to NHM (p= 0.0152; 48 hrs; n=3) (Figure 22).

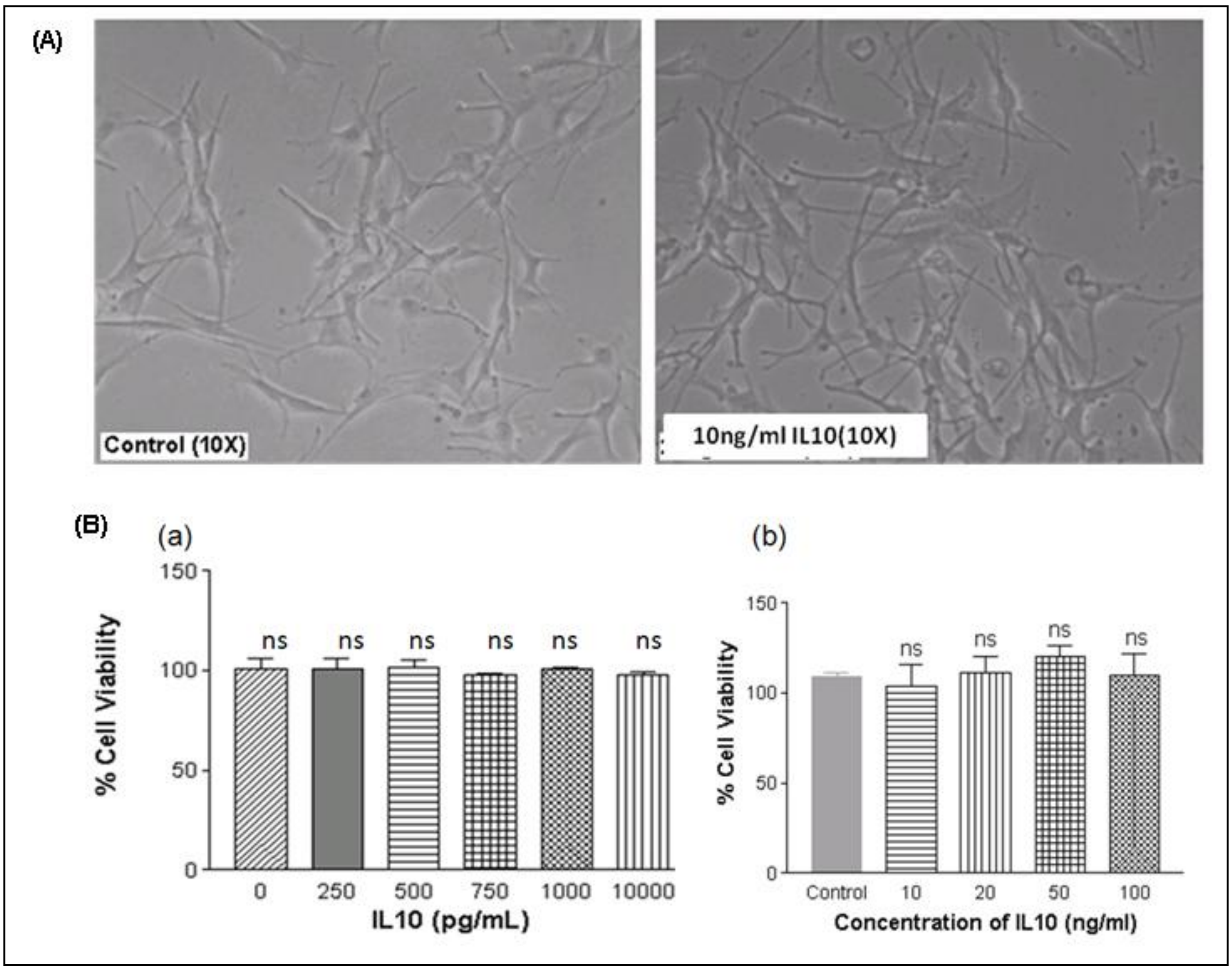

Figure 20: Effect of IL-10 on cell death of NHM: Effect of IL-10 stimulation on NHM morphology (Magnification: 10X; Scale: 100μm).The NHM cells were treated with IL-10

(0.25-10ng/ml) for 48 hrs and Mean % cell viability was shown at 48 hrs. IL-10 did not affect growth and viability of NHM (n=3, *p*=0.075).

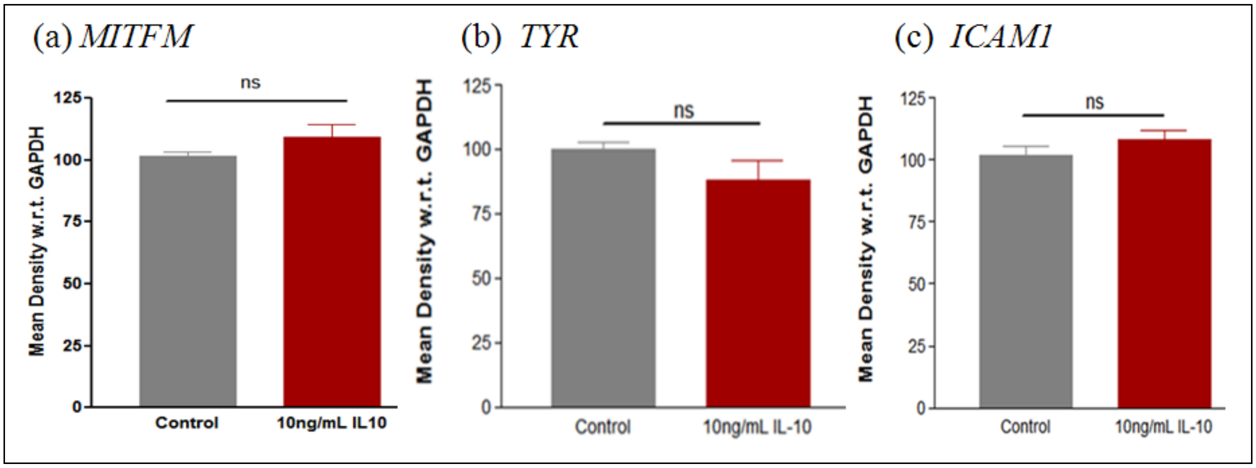

Figure 21: Effect of IL10 on *MITF-M, TYR* and *ICAM1* transcript levels in NHM: No significant effect was observed for *MITF-M* (*p*= 0.2401), *TYR (p* = 0.2934) and *ICAM1 (p* = 0.3608) transcript levels upon IL-10 treatment on NHM (n=3, 48 hrs treatment).

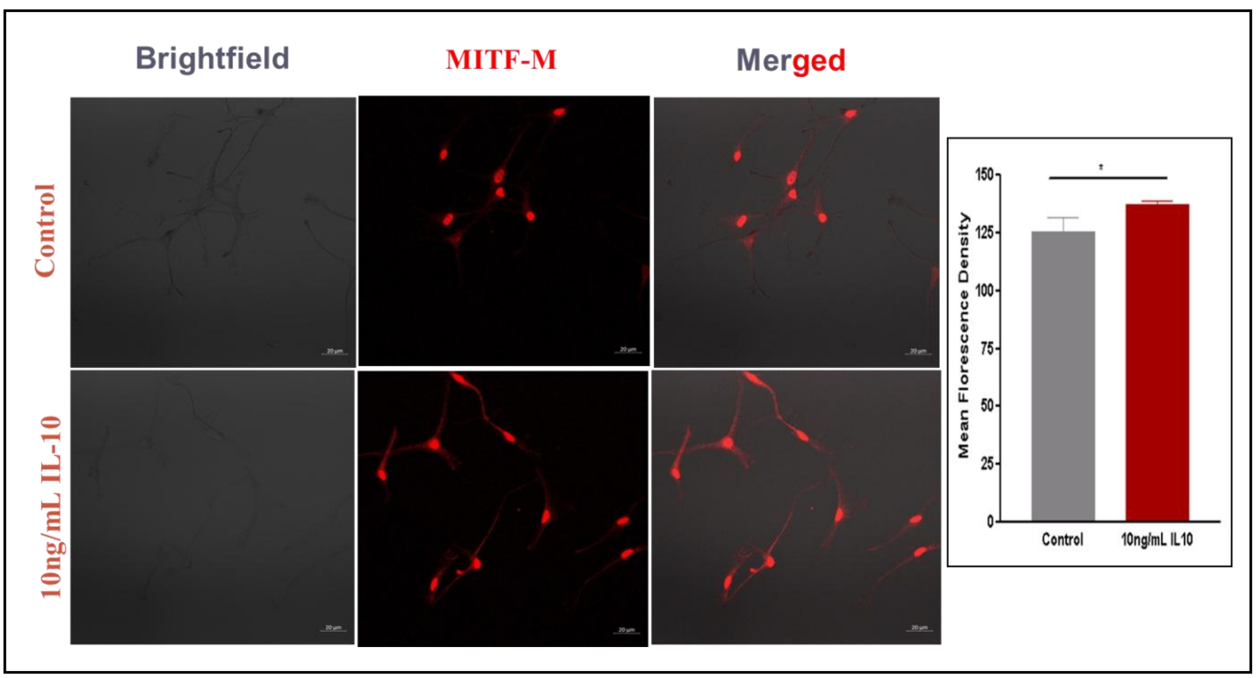

Figure 22: Analysis of MITF-M levels in NHM upon IL-10 treatment by Immunofluorescence: Treatment with IL-10 (10ng/mL) caused significant increase (*p*= 0.0152) in MITF-M protein expression levels (n=3).

4.3.6 Combinatorial effect of cytokines on NHM viability:

TNF-α, IL-1α, and IL-6 caused a dose dependent decrease in cell viability of cultured melanocytes. However, IL-10 did not show any significant alteration in growth and viability of cultured melanocytes. All cytokines in synergism with high H_2O_2 environment may lead to enhanced compromised state of melanocytes, affecting overall survival and homeostasis of melanocytes. Hence, we have treated NHM with various combinations of cytokines.

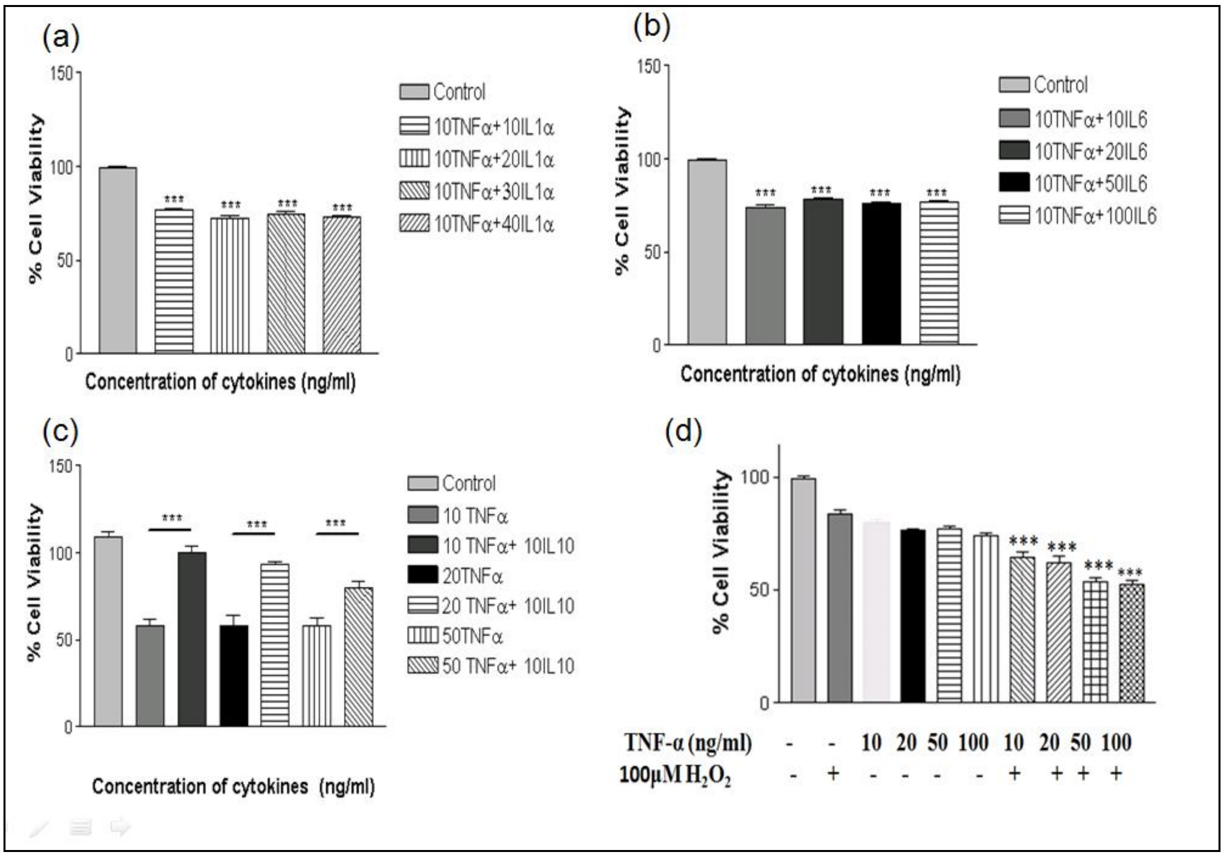

Figure 23: Combinatorial effect of cytokines on NHM viability: (a, b) Synergistic effect of TNF-α along with IL-1α, IL-6 and (c) antagonistic effect of IL-10 on NHM viability in a dose dependent manner was observed. (d) Also, synergistic effect of TNF-α and H_2O_2 on NHM viability was observed.

4.4 DISCUSSION

Melanocytes are neural crest derived cells residing at the basal layer of the epidermis. Melanocyte survival and proliferation seem to be strongly correlated with expression of various factors such as cytokines secreted by keratinocytes, α-MSH, SCF etc. that govern the signaling pathways mediating differentiation and proliferation of melanocytes. Vitiligo is an acquired, progressive, hypomelanotic skin disorder manifested by selective destruction of melanocytes. Melanin pigment is a potent UV absorbent with antioxidant and radical scavenging properties and thus epidermal pigmentation is a major protective factor against genotoxic damage by UV radiation (Lin and Fischer, 2007).

As the top-most layer of the skin is mainly made up of dead cells, an increase in the thickness of the epidermis may occur as a combative measure against UV penetrance. Due to epidermal thickening, the skin acts as a barrier for epidermal somatic cell protection from the mutagenic effects of UV radiation. Earlier studies postulate development of epidermal hyperplasia, such as hyperkeratosis and acanthosis as a means of compensation for the absence of pigmentation in vitiligo skin (Jung *et al.,* 2015; El-Khateeb *et al.*, 2011; Awad, 2012). Inflammatory changes in the disturbed skin environment are more profound and intense and reflected in degenerative changes in melanocytes, vacuolar changes of basal cells, epidermal infiltration of lymphocytes, dermal infiltration of lymphocytes, and melanophages in the upper dermis (Hann *et al.,* 1992). Diminished melanocyte proliferation and melanogenesis can be correlated to the loss of rete-ridges in the basal skin layer where the melanocytes reside and proliferate. In our study, we found significant increase in the thickening of the viable epidermis in lesional skin of patients compared to control skin (Figs 1 and 2) which are in accordance with the previous reports (Jung *et al.*, 2015; El-Khateeb *et al.*, 2011; Awad, 2012). An interesting finding of our present study is the significant thickening of lesional skin as compared to non-lesional and control skin, postulating importance of the microenvironment of thickened skin in the hypomelanotic patches of skin. Vitiligo patients showed reduced expression of *MITF-M* gene in perilesional *vs.* lesional and, lesional as well as non lesional skin when compared to controls (Kingo *et al*., 2008). This is in accordance with our results where we found significant decrease in MITF-M protein expression in lesional and non-lesional skin when compared to control skin samples (Figs 3 and 4).

Dysregulation of production of cytokines or their action plays a central role in the development of autoimmunity (O'Shea, 2002). In the epidermal melanin unit, the keratinocyte derived cytokines TNF-α, IL1-α, IL-6 act as paracrine inhibitors of melanocyte proliferation and melanogenesis (Swope *et al*., 1991). The epidermal as well as systemic cytokine imbalance have been reported in vitiligo patients including higher TNF-α, IL-6, IL-1α and IL1-β levels (Moretti *et al*., 2002, Laddha *et al*., 2012, Laddha *et al*., 2014, Tu *et al*., 2003, Birol *et al*., 2006, Singh *et al*., 2012). Our results showed significant decrease in melanocyte viability upon treatment with TNF-α, IL-6, IL-1α in a dose dependent manner (Figs 5, 14 and 17). However, IL-10 was having non-significant effect on melanocyte viability. Interestingly, we found ameliorative effect of IL-10 on TNF-induced melanocyte viability; on the contrary TNF-α was exerting synergism with IL-6, IL-1α, and oxidative stress. All these conditions of increased oxidative stress, as well as cytokine imbalance were well evident in circulation and skin microenvironment of vitiligo patients. MITF is a master transcriptional regulator of melanogenesis and melanocyte survival and exerts its mechanism by regulating TYR, TYRP1, DCT etc. Our results showed a significant decrease in MITF-M levels on NHM upon TNF-α, IL-6, IL-1α treatment. Interestingly, we found IL-10 significantly increases MITF-M expression on NHM, suggesting an imbalance of pro and anti-inflammatory cytokines in the regulation of master transcriptional regulator of melanogenesis. Various studies reported down regulation of MITF-M and melanogenesis in melanocytes by treatment with IL-17A, IL-1β, IL-6, and TNF-α (Kamaraju *et al*., 2002; Kotobuki *et al*., 2012; Choi *et al*., 2005) which are in the line of our findings. TYR and TYRP1 are the target genes of MITF-M and catalyse the rate limiting steps of melanin synthesis and we found down regulation of *TYR* by TNF-α and IL-6 treatment. IL-1α ($3x10^{-14}$ M) was found to decrease *MITF-M* expression and showed an inhibitory effect on tyrosinase activity in melanocytes (Swope *et al*.,1991). The MITF transcriptional activity is also dependent on its phosphorylation state (Hemesath *et al*., 1998). Therefore, the inhibitory effect of IL-1α might regulate tyrosinase function rather than its transcription. *TYRP1* gene encodes a melanosomal enzyme that belongs to the tyrosinase family and plays an important role in the melanin biosynthetic pathway (Cui *et al*., 2015). No significant difference was observed in the *TYRP1* levels similar to tyrosinase, upon IL-1α stimulation of NHM.

Both IL-1α and IL1-β can self-regulate their expression which serves as a positive-feedback loop that amplifies the IL1 response in an autocrine or paracrine manner (Hu *et al*., 2003). In contrast, IL1-β produced by different cell types including tissue macrophages and skin dendritic cells was reported to activate complement components and other cytokines including IL1 itself (Dinarello *et al*., 2011). Interestingly, in the present study, both *IL1A* and *IL1B* were found to be significantly upregulated upon IL1 stimulation in NHM (Figure 18). IL1RN is a specific inhibitor of the activity of both IL-1α and IL1-β. IL-1RN binds tightly to IL1RI and blocks the activity of either IL-1α or IL1-β. Cell activation by IL1 is mediated exclusively by IL1R1 and requires IL1 receptor accessory protein for cell signaling (Boraschi *et al*., 2006, Jacques *et al*., 2006). On the contrary, IL1R2 has no signaling properties, and appears to act merely as a 'decoy receptor' (Martin *et al*., 2002; Dunne *et al*., 2003). Bellehumeur *et al*., (2009) have reported the regulation of IL1R1, IL1R2, and IL1RN by IL1-β in human endometrial cells. Our results showed increased *IL1RN* transcript levels upon IL-1α stimulation in NHM. In addition, IL-1α is reported to stimulate *IL1*, *TNF-A*, and *IL-6* expression in human cardiac myofibroblasts (Turner *et al*., 2007). We observed upregulation of *IL1RN*, *IL1A*, *IL1B*, *IL6*, *TNFA* and *ICAM1* and down regulation of *MITF-M* upon exogenous IL-1α stimulation in NHM (Figure 18), suggesting its regulatory role in melanocyte homeostasis in vitiligo. Both TNF-α and IL1-β were reported to stimulate IL8 release from melanocytes (Miniati *et al*., 2014), whereas in the present study we did not find any effect of IL-1α on IL8 production in NHM (Figure 18). IL8 is an important chemokine produced by monocytes, mast cells, fibroblasts, endothelial cells, dendritic cells and keratinocytes in inflammatory skin diseases. IL8 is chemotactic for neutrophils, T-lymphocytes, basophils, and keratinocytes (Luger *et al*., 1990). ICAM1 is important for activating T-cells and recruiting leukocytes (Hedley *et al*., 1998). Beyond its classically described function as an adhesion and viral entry molecule, ICAM1 on the surface of T-cells participates in signal transduction affecting several T-cell functions, including activation, proliferation, cytotoxicity, and cytokine production and thereby plays an important role in modulating autoimmune diseases (Stanciu *et al*., 1998). Earlier our lab reported increased expression of *ICAM1*, *IFNG* and *TNFB*, along with decreased cytotoxic

T-lymphocyte associated antigen-4 (*CTLA4*) and decreased T reg cells in vitiligo patients (Laddha *et al*., 2012, Laddha *et al*., 2013, Dwivedi *et al*., 2013, Dwivedi *et al*., 2011, Dwivedi *et al*., 2013). Increased IFN-γ levels in vitiligo patients lead to increased *ICAM1* expression which can be a probable link between cytokines and T-cell involvement in the pathogenesis of vitiligo (Dwivedi *et al*., 2013). TNF-α is reported to induce IL1-α, IL1-β and IL-6 synthesis in glioma cells and cardiac fibroblasts (Turner *et al*., 2007). In addition, TNF-α in the presence of IFN-γ modulates IL6 and its receptor in human monocytic cells (Sanceau *et al*., 1991). Interestingly, we found IL-1α to induce IL6 expression in NHM at 100 ng/ml (Figure 18).

IL-1α was reported to be cytostatic rather than cytotoxic on NHM (Swope *et al*., 1991). The present study also showed a significant decrease in cell viability of NHM with reduced growth upon exogenous IL-1α stimulation suggesting the role of IL-1α in melanocyte destruction in vitiligo. The blockade of IL1 by Anakinra, a recombinant IL1RN which affects the biological activity of naturally occurring IL1 by competitively inhibiting the binding of IL1 to IL1R1 has been implicated to control various autoimmune disorders including inflammation and rheumatoid arthritis, juvenile idiopathic arthritis (Mertens *et al*., 2009, Pascual *et al*., 2005). Protective effect of IL1-β monoclonal antibody in insulin-producing beta cells is reported in type 2 diabetic patients (Donath *et al*., 2008). TNF-α, IL-1α and IL-6 induce ICAM-1 expression in melanocytes, thus promoting melanocyte-leukocyte attachment. This might explain the selective destruction of vitiliginous melanocytes (Yohn *et al*., 1990). Previously, we reported increased *ICAM-1* expression in vitiligo patients (Dwivedi *et al*., 2013). Interestingly, we also found induction of *ICAM1* expression upon IL-6 treatment in melanocytes. Toosi *et al*., (2012) have reported that exposure of vitiligo inducing phenols (4-tertiary butyl phenol and mono-benzyl ether of hydroquinone) to NHM increased the expression of *XBP1*, further activating IL6 and IL8 production by melanocytes.

Our results indicated increased levels of *TNFA* in vitiligo skin (lesional and non lesional). Exogenous stimulation of TNF-α on melanocytes caused significant decrease in viability, significant increase in cellular and mitochondrial ROS levels, ~20% decrease in mitochondrial complex1 activity, decrease in melanin content *via* shedding of dendrites and down regulation of *MITF-M*, *TYR* and increased *TNFR1, IL6, ICAM1* expression while *TNFR2* levels remained unaltered (Fig 10). Upon TNF-α stimulation, LC3I-II conversion at 12 hrs and caspase-8 activation at 48 hrs were observed, which disappeared at 48 hrs and 24 hrs respectively (Figs 12 and 13). All these studies advocate the crucial role of TNF-α in melanocyte homeostasis and autoimmune pathogenesis of vitiligo. On the contrary to pro-inflammatory cytokines, IL-10 showed non-significant effect on NHM viability, *TYR*, *MITF-M* and *ICAM-1* transcript levels, but increased the MITF-M protein expression and ameliorates TNF-α induced cytotoxicity.

In conclusion, candidate cytokines addressed in the present study i.e., TNF-α, IL-1α, IL-6 and IL-10 found to regulate melanogenesis and proliferation of NHM. Overall, the present study along with other existing reports advocate the therapeutic potential of low cytokine dose therapy in amelioration of vitiligo. Thus, this will pave the way for better understating and designing of personalized treatment modality for vitiligo.

4.5 REFERENCES

- Al Badri, A.M.T., Todd, P.M., Garioch, J.J., Gudgeon, J.E., Stewart, D.G. and Goudie, R.B., 1993. An immunohistological study of cutaneous lymphocytes in vitiligo. *The Journal of pathology*, *170*(2), pp.149-155.
- Awad, SS. (2012). Dermabrasion may repigment vitiligo through stimulation of melanocyte precursors and elimination of hyperkeratosis.*Journal of cosmetic dermatology*, *11*, 318-322.
- Baker, J.R., 1962. Experiments on the action of mordants 2. Aluminium-haematein. *Journal of Cell Science*, *3*(64), pp.493-517.
- Bellehumeur, C., Blanchet, J., Fontaine, J.Y., Bourcier, N. and Akoum, A., 2009. Interleukin 1 regulates its own receptors in human endometrial cells via distinct mechanisms. *Human reproduction*, *24*(9), pp.2193-2204.
- Birol, A., Kisa, U., Kurtipek, G.S., Kara, F., Kocak, M., Erkek, E. and Caglayan, O., 2006. Increased tumor necrosis factor alpha (TNF-α) and interleukin 1 alpha (IL1α) levels in the lesional skin of patients with nonsegmental vitiligo. *International journal of dermatology*, *45*(8), pp.992-993.

- Boraschi, D. and Tagliabue, A., 2006. The interleukin-1 receptor family.*Vitamins & Hormones*, *74*, pp.229-254.
- Choi, H., Ahn, S., Lee, B.G., Chang, I. and Hwang, J.S., 2005. Inhibition of skin pigmentation by an extract of Lepidium apetalum and its possible implication in IL-6 mediated signaling. *Pigment Cell & Melanoma Research*, *18*(6), pp.439-446.
- Cui, T.T., Yi, X.L., Zhang, W.G., Wei, C., Zhou, F.B., Jian, Z., Wang, G., Gao, T.W., Li, C.Y. and Li, K., 2015. miR-196a-2 rs11614913 polymorphism is associated with vitiligo by affecting heterodimeric molecular complexes of Tyr and Tyrp1. *Archives of dermatological research*, *307*(8), pp.683-692.
- Dinarello, C.A., 2011. Interleukin-1 in the pathogenesis and treatment of inflammatory diseases. *Blood*, *117*(14), pp.3720-3732.
- Donath, M.Y. and Mandrup-Poulsen, T., 2008. The use of interleukin-1-receptor antagonists in the treatment of diabetes mellitus. *Nature Reviews. Endocrinology*, *4*(5), p.240.
- Dunne, A. and O'Neill, L.A., 2003. The interleukin-1 receptor/Toll-like receptor superfamily: signal transduction during inflammation and host defense. *Sci. STKE*, *2003*(171), pp.re3-re3.
- Dwivedi, M., Laddha, N.C., Arora, P., Marfatia, Y.S. and Begum, R., 2013. Decreased regulatory T-cells and CD4+/CD8+ ratio correlate with disease onset and progression in patients with generalized vitiligo.*Pigment cell & melanoma research*, *26*(4), pp.586-591.
- Dwivedi, M., Laddha, N.C., Imran, M., Shah, B.J. and Begum, R., 2011. Cytotoxic T-lymphocyte-associated antigen-4 (CTLA-4) in isolated vitiligo: a genotype-phenotype correlation. *Pigment cell & melanoma research*,*24*(4), pp.737-740.
- Dwivedi, M., Laddha, N.C., Shah, K., Shah, B.J. and Begum, R., 2013. Involvement of interferon-gamma genetic variants and intercellular adhesion molecule-1 in onset and progression of generalized vitiligo.*Journal of Interferon & Cytokine Research*, *33*(11), pp.646-659.
- El-Khateeb, EA, Ragab, NF, Mohamed, SA. (2011). Epidermal photoprotection: comparative study of narrowband ultraviolet B minimal erythema doses with and

without stratum corneum stripping in normal and vitiligo skin. *Clinical and experimental dermatology*, *36*, 393-398.

- Hann, SK, Chun, WH. (2000). Autocytotoxic Hypothesis for the Destruction of Melanocytes as the Cause of Vitiligo. *Vitiligo: A Monograph on the Basic and Clinical Science*, 137.
- Hedley, S.J., Metcalfe, R., Gawkrodger, D.J., Weetman, A.P. and Mac Neil, S., 1998. Vitiligo melanocytes in long-term culture show normal constitutive and cytokine-induced expression of intercellular adhesion molecule-1 and major histocompatibility complex class I and class II molecules. *British Journal of Dermatology*, *139*(6), pp.965-973.
- Hemesath, T.J., Price, E.R., Takemoto, C., Badalian, T. and Fisher, D.E., 1998. MAP kinase links the transcription factor Microphthalmia to c-Kit signalling in melanocytes. *Nature*, *391*(6664), p.298.
- Hu, D.N., 2008. Methodology for evaluation of melanin content and production of pigment cells in vitro. *Photochemistry and photobiology*,*84*(3), pp.645-649.
- Imran, M., Laddha, N.C., Dwivedi, M., Mansuri, M.S., Singh, J., Rani, R., Gokhale, R.S., Sharma, V.K., Marfatia, Y.S. and Begum, R., 2012. Interleukin-4 genetic variants correlate with its transcript and protein levels in patients with vitiligo. *British Journal of Dermatology*, *167*(2), pp.314-323.
- Jacques, C., Gosset, M., Berenbaum, F. and Gabay, C., 2006. The role of IL-1 and IL-1Ra in joint inflammation and cartilage degradation. *Vitamins & Hormones*, *74*, pp.371-403.
- Jung, SE, Kang, HY, Lee, ES, Kim, YC. (2015). Changes of epidermal thickness in vitiligo. *The American Journal of Dermatopathology*, *37*, 289-292.
- Kamaraju, A.K., Bertolotto, C., Chebath, J. and Revel, M., 2002. Pax3 down-regulation and shut-off of melanogenesis in melanoma B16/F10. 9 by interleukin-6 receptor signaling. *Journal of Biological Chemistry*, *277*(17), pp.15132-15141.
- Kingo, K., Aunin, E., Karelson, M., Rätsep, R., Silm, H., Vasar, E. and Kõks, S., 2008. Expressional changes in the intracellular melanogenesis pathways and their possible role the pathogenesis of vitiligo. *Journal of dermatological science*, *52*(1), pp.39-46.

- Kotobuki, Y., Tanemura, A., Yang, L., Itoi, S., Wataya-Kaneda, M., Murota, H., Fujimoto, M., Serada, S., Naka, T. and Katayama, I., 2012. Dysregulation of melanocyte function by Th17-related cytokines: significance of Th17 cell infiltration in autoimmune vitiligo vulgaris. *Pigment cell & melanoma research*, *25*(2), pp.219-230.
- Laddha, N.C., Dwivedi, M. and Begum, R., 2012. Increased Tumor Necrosis Factor (TNF)-α and its promoter polymorphisms correlate with disease progression and higher susceptibility towards vitiligo. *PLoS One*,*7*(12), p.e52298.
- Laddha, N.C., Dwivedi, M., Gani, A.R., Mansuri, M.S. and Begum, R., 2013. Tumor Necrosis Factor B (TNFB) genetic variants and its increased expression are associated with vitiligo susceptibility. *PloS one*, *8*(11), p.e81736.
- Laddha, N.C., Dwivedi, M., Mansuri, M.S., Singh, M., Patel, H.H., Agarwal, N., Shah, A.M. and Begum, R., 2014. Association of neuropeptide Y (NPY), interleukin-1B (IL1B) genetic variants and correlation of IL1B transcript levels with vitiligo susceptibility. *PloS one*, *9*(9), p.e107020.
- Lin, J.Y. and Fisher, D.E., 2007. Melanocyte biology and skin pigmentation. *Nature*, *445*(7130), p.843.
- Lotti, T., Hercogova, J., Wollina, U., Chokoeva, A.A., Zarrab, Z., Gianfaldoni, S., Roccia, M.G., Fioranelli, M. and Tchernev, G., 2015. Vitiligo: successful combination treatment based on oral low dose cytokines and different topical treatments. *Journal of biological regulators and homeostatic agents*, *29*(1 Suppl), pp.53-58.
- Luger, T.A. and Schwarz, T., 1990. Evidence for an epidermal cytokine network. *Journal of Investigative Dermatology*, *95*(6), pp.S100-S104.
- Martin, M.U. and Wesche, H., 2002. Summary and comparison of the signaling mechanisms of the Toll/interleukin-1 receptor family.*Biochimica et Biophysica Acta (BBA)-Molecular Cell Research*, *1592*(3), pp.265-280.
- Mertens, M. and Singh, J.A., 2009. Anakinra for rheumatoid arthritis: a systematic review. *The Journal of rheumatology*, *36*(6), pp.1118-1125.
- Miniati, A., Weng, Z., Zhang, B., Therianou, A., Vasiadi, M., Nicolaidou, E., Stratigos, A.J., Antoniou, C. and Theoharides, T.C., 2014. Stimulated human melanocytes

express and release interleukin-8, which is inhibited by luteolin: relevance to early vitiligo. *Clinical and experimental dermatology*, *39*(1), pp.54-57.

- Moretti, S., Fabbri, P., Baroni, G., Berti, S., Bani, D., Berti, E., Nassini, R., Lotti, T. and Massi, D., 2009. Keratinocyte dysfunction in vitiligo epidermis: cytokine microenvironment and correlation to keratinocyte apoptosis.*Histology and histopathology*, *24*(7), p.849.
- Moretti, S., Spallanzani, A., Amato, L., Hautmann, G., Gallerani, I., Fabiani, M. and Fabbri, P., 2002. New insights into the pathogenesis of vitiligo: imbalance of epidermal cytokines at sites of lesions. *Pigment Cell & Melanoma Research*, *15*(2), pp.87-92.
- Mosmann, T., 1983. Rapid colorimetric assay for cellular growth and survival: application to proliferation and cytotoxicity assays. *Journal of immunological methods*, *65*(1-2), pp.55-63.
- O'Shea, J.J., Ma, A. and Lipsky, P., 2002. Cytokines and autoimmunity. Nature Reviews Immunology, 2(1), pp.37-45.
- Pascual, V., Allantaz, F., Arce, E., Punaro, M. and Banchereau, J., 2005. Role of interleukin-1 (IL-1) in the pathogenesis of systemic onset juvenile idiopathic arthritis and clinical response to IL-1 blockade. *Journal of Experimental Medicine*, *201*(9), pp.1479-1486.
- Prajapati, P., Sripada, L., Singh, K., Bhatelia, K., Singh, R. and Singh, R., 2015. TNF-α regulates miRNA targeting mitochondrial complex-I and induces cell death in dopaminergic cells. *Biochimica et Biophysica Acta (BBA)-Molecular Basis of Disease*, *1852*(3), pp.451-461.
- Sanceau, J., Wijdenes, J., Revel, M. and Wietzerbin, J., 1991. IL-6 and IL-6 receptor modulation by IFN-gamma and tumor necrosis factor-alpha in human monocytic cell line (THP-1). Priming effect of IFN-gamma. *The Journal of Immunology*, *147*(8), pp.2630-2637.
- Sevrioukova, I.F., 2011. Apoptosis-inducing factor: structure, function, and redox regulation. *Antioxidants & redox signaling*, *14*(12), pp.2545-2579.
- Singh, S., Singh, U. and Pandey, S.S., 2012. Serum concentration of IL-6, IL-2, TNF-α, and IFNγ in Vitiligo patients. *Indian journal of dermatology*, *57*(1), p.12.

- Stanciu, L.A. and Djukanovic, R., 1998. The role of ICAM-1 on T-cells in the pathogenesis of asthma. *European Respiratory Journal*, *11*(4), pp.949-957.
- Swope, V.B., Abdel-Malek, Z., Kassem, L.M. and Nordlund, J.J., 1991. Interleukins 1α and 6 and tumor necrosis factor-α are paracrine inhibitors of human melanocyte proliferation and melanogenesis. *Journal of investigative dermatology*, *96*(2), pp.180-185.
- Taieb, A. and Picardo, M., 2007. The definition and assessment of vitiligo: a consensus report of the Vitiligo European Task Force. *Pigment Cell & Melanoma Research*, *20*(1), pp.27-35.
- Tanabe, K., Matsushima-Nishiwaki, R., Yamaguchi, S., Iida, H., Dohi, S. and Kozawa, O., 2010. Mechanisms of tumor necrosis factor-α-induced interleukin-6 synthesis in glioma cells. *Journal of neuroinflammation*,*7*(1), p.16.
- Thomas J. Kindt.,2007. *Kuby Immunology (6th Edition).*
- Toosi, S., Orlow, S.J. and Manga, P., 2012. Vitiligo-inducing phenols activate the unfolded protein response in melanocytes resulting in upregulation of IL6 and IL8. *Journal of Investigative Dermatology*,*132*(11), pp.2601-2609.
- Tu, C.X., Gu, J.S. and Lin, X.R., 2003. Increased interleukin-6 and granulocyte–macrophage clony stimulating factor levels in the sera of patients with non-segmental vitiligo. *Journal of dermatological science*,*31*(1), pp.73-78.
- Turner, N.A., 2011. Therapeutic regulation of cardiac fibroblast function: targeting stress-activated protein kinase pathways. *Future cardiology*,*7*(5), pp.673-691.
- Turner, N.A., Mughal, R.S., Warburton, P., O'Regan, D.J., Ball, S.G. and Porter, K.E., 2007. Mechanism of TNFα-induced IL-1α, IL-1β and IL-6 expression in human cardiac fibroblasts: effects of statins and thiazolidinediones. *Cardiovascular research*, *76*(1), pp.81-90.
- Yohn, J.J., Critelli, M., Lyons, M.B. and Norris, D.A., 1990. Modulation of melanocyte intercellular adhesion molecule-1 by immune cytokines.*Journal of investigative dermatology*, *95*(2), pp.233-237.